# Underwater Optical Imaging: The Past, the Present, and the Prospects

Jules S. Jaffe, *Associate Member, IEEE*

***Abstract*—This paper discusses the current state of underwater optical imaging in the context of physics, technology, biology, and history. The paper encompasses not only the history of human's ability to see underwater, but also the adaptations that various organisms living in oceans or lakes have developed. The continued development of underwater imaging systems at military, commercial, and consumer levels portends well for both increased visibility and accessibility by these various segments. However, the fundamental limits imposed by the environment, as currently understood, set the ultimate constraints. Physics, biology, computer modeling, processing, and the development of technology that ranges from simple cameras and lights to more advanced gated and modulated illumination are described. The future prospects for continuing advancements are also discussed.**

***Index Terms*—Underwater optical imaging.**

## I. Introduction

IT is not entirely clear when life originated approximately 3.5–4 billion years ago, whether it was in the surface of the oceans, hot springs on land, or in the deeper sea. However, what is clear is that the ability to harvest the energy of the sun quickly became the preferred way to survive and proliferate in a nutrient rich world, where the basic building blocks of life could be found and employed for reproduction. In addition, as some of these primordial organisms evolved, their ability increased so that they not only could use the light energy to create carbon-based, macromolecules but also to sense the environment. Evidence that this is true comes from a retrospective examination of the downwelling spectra of water [1], depicted in Fig. 1(a), when compared to the sensitivity of the vertebrate eye as in Fig. 1(b). It is clear that the transparency of ocean water provides a "window of opportunity" for both harvesting energy and perceiving the world. There is no doubt that it provides the basis for almost all life on Earth.

The general definition of "image" embodies the idea that light has been sensed from a multiplicity of directions, whether simultaneously or sequentially to produce a vector quantity, the intensity of the electromagnetic field as a function of direction: $I(\theta, \varphi)$. The evolutionary development and migration from a simple "sensing organ" to one that can perceive images is commensurate with the migration from a single light receptor to the more complex anatomy of multiple receivers that can simultaneously sense light from multiple directions that led to the first, albeit primitive, images. Fig. 2, reproduced from [2], illustrates a number of underwater light sensing and imaging systems that go from simple direction sensing to fully developed imaging systems.

A survey of underwater animal vision provides evidence for a variety of fascinating adaptations that include low-light vision, extreme spectral resolution, a high level of visual acuity, and the capability to sense polarized light. The contemporary view, in the context of survival, is that these adaptations are important for finding food and conspecifics to mate with while avoiding predators. All of this is in an aqueous environment whose upper waters are daily lit by the sun and subject to a variety of effects that modulate the properties of the water and, hence, the capability for using vision.

As man eventually wandered back into the sea, equipped with an optical imaging system that was optimized to work in air, underwater vision became feasible via the imposition of a flat plate between the human eye and the water. The first attempt at seeing underwater as documented in [3] was in 1405 when Konrad Kyeser fashioned a leather diving suit (whose idea is attributed to Roger Bacon) with two glass windows. Henceforth, a number of underwater observations commenced, first from underwater submersibles, then to diving suits that were connected to a surface air source with the eventual observation by an untethered human using the aqualung. The 19th and early 20th century saw the incorporation of the advances in land-based technology that used 35-mm film instead of glass plates. Commensurate developments in underwater housings that could accommodate both cameras and lights permitted the observation of the underwater environment at night. This greatly facilitated the progress of marine biology, as many important adaptations occur during both crepuscular times (dusk and dawn) and a range of underwater lighting environments that go from a full-lit moon, to a moonless sky.

The modern era of underwater imaging, as defined here, arose when electronic imaging systems were developed. The first systems used variations on vacuum tubes with analog transmission from the imaging system to both viewing and recording devices. Further evolution to digital imaging with the invention of the charge-coupled device (CCD) camera and the progression of

Manuscript received May 31, 2014; accepted August 15, 2014. Date of publication October 20, 2014; date of current version July 10, 2015. This work was supported by the National Science Foundation, the U.S. Office of Naval Research, the Seaver Foundation, J. Beyster, S. and B. Kimmich, and the Keck Foundation.

**Associate Editor: N. Ross Chapman**.

The author is with the Marine Physical Lab, Scripps Institution of Oceanography, University of California San Diego, La Jolla, CA 92093-0238 USA (e-mail: jjaffe@ucsd.edu).

Digital Object Identifier 10.1109/JOE.2014.2350751

0364-9059 © 2014 IEEE. Translations and content mining are permitted for academic research only. Personal use is also permitted, but republication/redistribution requires IEEE permission. See http://www.ieee.org/publications_standards/publications/rights/index.html for more information.

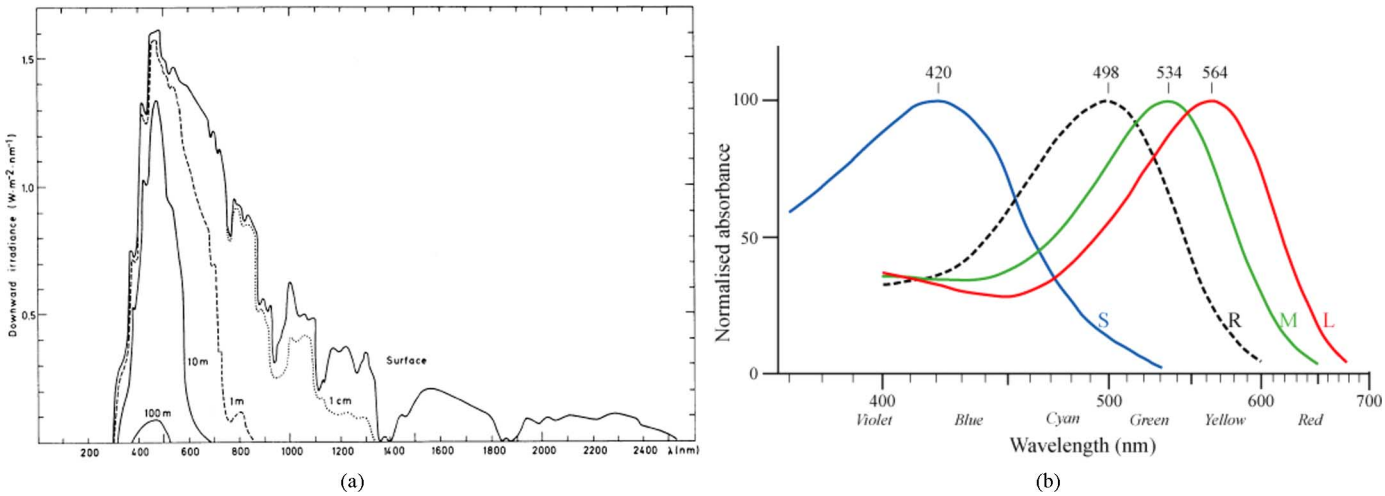


Fig. 1. (a) Spectra of daily downward irradiance in seawaters at various depths in the ocean over a broad spectral range [1]. (b) Normalized sensitivity of the photoreceptors in the vertebrate eye: black = rods; blue, green, red = cones [2].

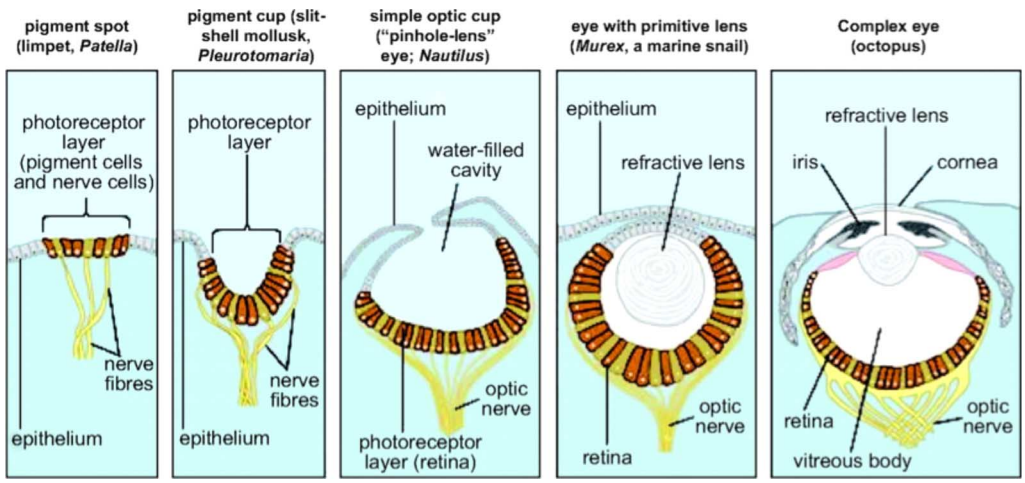


Fig. 2. Progression of underwater animal optical imaging systems that go from simple direction finding (left) to imaging (right) [2].

such devices to the nearly quantum limited performance that we see today, availed underwater imagers with increasingly sophisticated hardware. The development of computers for postprocessing recorded images facilitated both contrast and resolution enhancement of the many, necessarily poor, pictures that were taken.

Advances in sensing technology were also accompanied by simultaneous advances in the production of light. This included the development of strobe lights, instead of the combustible powder used in the earliest pictures, to various types of lights such as mercury vapor and halogens. The development of lasers facilitated the use of more sophisticated systems that require either highly collimated or coherent beams. Advances in lighting presently continue, with the proliferation of light emitting diodes that have increased electro–optic efficiency with a commensurate range of spectral choices.

Note that a number of reviews of underwater imaging have been published in the last decades. A former review [4], necessarily briefer than this one, reconciled both the physics and optics with what was then the current state of the art. In the interim, several reviews of the history of optical imaging [3] and technological developments have appeared [5]–[7]. Given the rapid increase in electro–optic technology, there is no doubt that this will not be the last one.

## II. Light and the Underwater Environment

### A. Light Propagation in 3-D

The fundamental physics of light are well understood and will only be considered briefly in the context of underwater imaging. Modern physics characterizes light as both a wave that can be subject to diffraction and coherent superposition as well as a particle; a photon, as evidenced by the photoelectric effect, is packaged in a quantum. This paper will reflect this duality in referring to both "photon scatter" as well as the propagation of the "light wave."

The propagation of light follows from a solution of the wave equation as unified by Maxwell in the 1860s. Here, we address

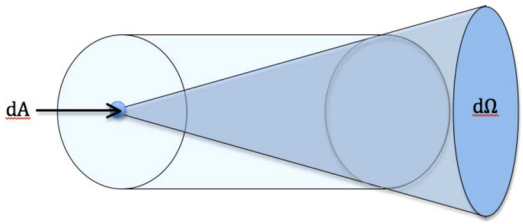


Fig. 3. Gershun's tube: Radiance is defined as the flux of optical energy integrated over area $dA$ that is incident from a cone of solid angle $d\Omega$ whose boundary is delineated by the tube, as shown.

only the electric field as conveniently represented by its two orthogonal components $E_x$ and $E_y$ oscillating with phase offset $\delta$. Envisioning a collection of such propagating waves, the distribution of the resultant electromagnetic field can be characterized using these vectors and their relative synchronization as described by their phase offset. The Stokes vector $[I, Q, U, V] =$ [total radiation, horizontally linearly polarized, oblique $(\pi/4)$ linearly polarized, circularly polarization] characterizes the polarization "state" in considering the aggregate of such individual particles or waves. Note that such a description describes the photon or wave propagation in only one propagation direction.

To fully describe the 3-D light field in aqueous media, it is necessary to characterize both directionality and intensity at every location. The radiant light field $L(\mathbf{r}, \theta, \varphi)$ is the intensity of light at position $\mathbf{r}$ propagating in a given $(\theta, \varphi)$ direction, per differential unit area per differential solid angle. Radiance is measured in W/m$^2$-sr. A convenient way to understand radiance is via the use of Gershun's tube [8], shown in Fig. 3, where a small area $(dA)$ measures the radiant flux incident over solid angle $d\Omega$ that has propagated through the tube that is shown. The radiant field in a 3-D environment can vary over space, time, and wavelength. Therefore, a complete description will be quite complicated, as it will also take into account, in addition to directionality, the intensity of the polarization components. Radiance, and its integration under some moment, or norm, of the radiant field, has played a fundamental role in underwater optics. A summary of these moments and their nomenclature can be found in well-known texts [1], [9], [10]. The most common measurement, scalar or vector irradiance, is but one example. A general introduction to underwater light propagation and several application areas governed by the basic physics can be found in [11].

### *B. Transmission of Light and the Physical Properties of the Environment*

In understanding the performance capability of underwater imaging systems, it is important to consider not only the source's radiance, but also the transformations the light incurs as it propagates through the medium. In a homogeneous ocean, the bulk property is governed by the complex index of refraction, $\widetilde{\eta} = \eta + i\kappa$, where the real part $\eta$ is related to the phase speed of the wave and the imaginary part $\kappa$ is related to the absorption loss. In a real ocean or lake, filled with myriad particles and properties, there is variability on every imaginable, and "local," scale. Here, light can be absorbed, refracted, reflected, scattered, and depolarized among other phenomena. Assuming a homogeneous media is, naturally, a simplification of the result of these interactions.

Considering bulk properties, the most commonly referenced are the attenuation and scattering of light in the more optically transparent window of the electromagnetic spectrum of 400–700 nm. Total light attenuation per meter $(c)$ consists of both the absorption $(a)$ and scatter $(b)$ that a photon may suffer when propagating from location $(r_0)$ to $(r)$ as described by the simple exponential law

$$I(r) = I(r_0)e^{-c(r-r_0)} = I(r_0)e^{-(a+b)(r-r_0)}. \quad (1)$$

Note also that $c^{-1}$ can also be regarded as the mean free path that a photon travels before being either scattered or attenuated [12]. The angular dependence of scatter is taken into account via $\beta(\theta, \varphi)$, the scattering function in the direction $(\theta, \varphi)$ that describes the scatter per unit meter, per unit steradian. Note that the function $\beta(\theta)$, as is commonly discussed, is derived from a circularly symmetric scatter function and, therefore, the scattering depends only on the angle theta, relative to the direction of scatter. The coefficient $b$ is a superposition of the many scattering events that occur in all directions, as expressed by the integral

$$b \equiv \int_0^{4\pi} \beta(\Psi)\delta\Omega = \int_0^{2\pi}\int_0^{\pi} \beta(\theta,\phi)\sin\theta d\theta d\phi = 2\pi\int_0^{\pi}\beta(\theta)\sin\theta d\theta \quad (2)$$

taken over all $4\pi$ steradians. As defined, the volume scattering (VSF), or phase function $\widetilde{\beta}(\theta)$, is a probability density function for scatter that quantifies the differential fraction of photons that will be scattered into solid angle $d\Omega$. As such, it is normalized to one

$$\frac{1}{4\pi}\int_{4\pi}\widetilde{\beta}(\theta)d\Omega = 1. \quad (3)$$

If polarization is neglected, or implicitly considered to be random, $a$, $b$, and $\beta(\theta)$ are a complete set of "bulk" environmental variables that can be used to understand and predict the propagation of light in homogeneous media. These quantities are referred to as the inherent optical properties (IOPs) and, as defined, they do not vary with the incident light field. Other properties, the apparent optical properties (AOPs), are dependent on the light field and are, therefore, subject to varying light conditions.

As a result of observing the properties of the underwater environment, various categorization schemes have been proposed. Among the most popular is the Jerlov-water-type classification [13] based on the spectral transmittance of downwelling irradiance in the surface waters (0–10 m). Categories go from type I water that is quite clear to type 9 that is strongly attenuating. A review of water mass classification can be found in [14] that credits the Secchi disk (to be discussed in Section IV) as the historical antecedent that contributed to the goal of optically classifying water types.

In addition to the measurement of $a$, $b$, and $c$, there have been a number of experiments to measure the VSF. A set of VSFs measured in the San Diego area [15] has been the stalwart of the oceanographic modeling community for many years and is shown in Fig. 4. Note that the forward scatter ($< 10^{\circ}$) is four to five orders of magnitude larger than the side ($\sim 90^{\circ}$) and backscatter ($\sim 180^{\circ}$). This is due to the prevalence of larger particles whose diameters are many optical wavelengths.

Recently, a number of commercial devices have been used to both measure the angular dependence of scatter and also invert that dependence for the particle size spectrum. The laser *in situ* scattering and transmissometry (LISST) device (Sequoia Scientific, Bellvue, WA, USA) is a multiangle scattering meter that has been used for measurement of flocculants and settling material [17] as well as to estimate both phytoplankton size and the effects of shape [18]. It is certainly an open issue as to how these VSFs change in space and time, however, there is strong indication that they are universally dominated by the small angle scatter, and hence, forward pointing.

A common way of classifying the transmission properties of the water is to refer to them as being either absorption or scatter dominated. The single scatter albedo, the ratio of $b/c$, quantifies the fraction of the total attenuation coefficient that is due to the total scatter coefficient $b$. Clear ocean waters are usually absorption limited with single scatter albedo values of 0.45, while murkier waters are typically scatter dominated where their single scatter albedo can be as high as 0.8

If polarization is included, the Muller matrix ($\boldsymbol{M}_{ij}$) describes the transformation of the Stokes vectors as the polarized light propagates from one location to another, so that

$$\begin{pmatrix} I' \\ Q' \\ U' \\ V' \end{pmatrix} = \begin{pmatrix} M_{11} & M_{12} & M_{13} & M_{14} \\ M_{21} & M_{22} & M_{23} & M_{24} \\ M_{31} & M_{32} & M_{33} & M_{34} \\ M_{41} & M_{42} & M_{43} & M_{44} \end{pmatrix} \begin{pmatrix} I \\ Q \\ U \\ V \end{pmatrix}$$

where the primes refer to the new location. There have been few measurements of the Muller matrix of oceanic water. One accomplished some time ago was by Voss and Fry [19]. As the authors state, the vast contribution was not from the aqueous seawater itself, but rather the constituents. Therefore, $\boldsymbol{M}$ is likely to vary as a function of location.

Oceanic turbulence is also a process that may affect the clarity of underwater images as the time-varying changes in refractive index can lead to both distortion and blurring [20]. Modeling of image formation in the presence of turbulence has also been considered [21].

There are also a variety of processes by which light can be converted from one wavelength to another. These processes are called "inelastic" in contrast to "elastic" as not all of the energy in the conversion process is absorbed by the daughter photon that emerges. The most common, fluorescence, is the result of the absorption of energy at one wavelength that is then converted and reemitted to another, longer wavelength. Raman scatter, the result of the photon giving its energy to a molecule that goes into a higher vibrational mode, results in the reemission of light at several wavelength bands both above and below the absorption.

## III. A Historical Recap of Underwater Optical Imaging

### A. Animal Systems for Underwater Imaging

Animal vision systems, evolved over several hundred million years of seeing in the ocean, provide a fascinating glimpse into some of the possibilities of underwater imaging. A recent trend in several research areas concerns biomimetrics, or how humans might emulate natural systems that have developed adaptations to accomplish certain goals. Although this has not yet influenced underwater imaging, the study of such systems yields both interesting science and may provide valuable hints to the development of future systems. Although a complete list of underwater organisms that use optical imaging is outside the scope of this paper, some special cases are discussed where unique and very interesting adaptations have occurred that meet the challenge of seeing underwater. This includes the use of multiple wavelengths, polarization, and low-light level sensitivity. We also note that to evade predators, a variety of strategies such as transparency and camouflage have been implemented to remain "cryptic" [22] so that the organisms are difficult to visually detect.

In this paper, we are concerned with two types of imaging; passive and active. In the case of passive imaging, the imager is not responsible for illumination. An example of passive imaging is the simple observation of objects in sunlit water.

In active imaging, the imager that senses the light is also responsible for the illumination. A simple underwater camera and strobe is an example. Since careful construction of beam patterns is important for preserving the contrast in underwater imaging, the design of underwater illumination sources plays an important role in optimizing underwater imaging system performance and is considered in substantial detail in this paper. In the case of biological imagers, for the most part, the imager is not illuminating the object of interest, so passive imaging is the main option.

To understand how passive imaging occurs using sunlight, the properties of the underwater ambient light field need to be understood. Fortunately, measurement of the underwater light field is commonplace in oceanography, primarily due to the important role that photosynthesis plays in global ecology [23]. The most traditional measurement in underwater light fields has been irradiance, however, with the recent proliferation of underwater radiometers [24], the prospects for systematic measurement of radiance have increased.

An early discovery in understanding underwater animal vision was that, since the cornea in animals in the sea is exposed to the water, the use of land optics does not work well. This is because the index of refraction between air and the cornea is large compared to that between seawater and the cornea. Fig. 5 illustrates the fact that underwater animals use graded index of refraction lenses to focus light onto the retina or light-sensitive organ [25].

Animal underwater vision systems can be characterized in the same way as any imaging system, the most important features being sensitivity, resolution, and contrast. Other interesting features are spectral bandwidth, and the ability to sense polarization. In the case of sensitivity, a large receiving aperture can be of distinct advantage, as it will hopefully integrate most of the

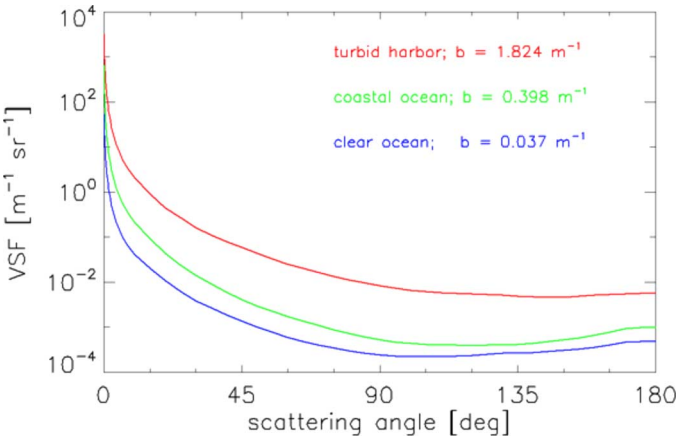


Fig. 4. Set of three volume scatter functions [16].

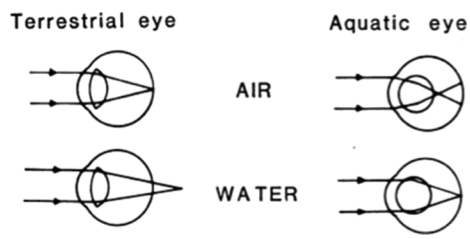


Fig. 5. Schematic of the geometric optical differences between a lens eye that is designed to operate in air and a lens eye that operates in water.

Fig. 6. Tempera painting from the 15th century depicting Alexander the Great in a clear diving bell that has been cast adrift by his wife and her lover. (Image courtesy of the J. Paul Getty Museum.)

light transiting through its aperture onto a few sensing elements providing higher signal-to-noise ratio (SNR) in low-light levels. As one example of large eyes, the eyes of giant and colossal squid can reach a diameter of 27 cm with a 9-cm pupil. A recent study [26] asserted that such an eye could detect a sperm whale at a range of 120 m in midwater (600–1000 m) depths. In this case, the authors argue that the detection occurs via the large aerial bioluminescence that is stimulated from the movement of the sperm whale through clouds of bioluminescent organisms. Another animal adapted to viewing in low-light levels is the bigeye tuna, *Thunnus obesus*. However, in this case, it is understood that the animal is hunting prey in the deepest lit depths as depth recorders tagged to the animals indicate that they can forage down to 500 m [27]

In the realm of other adaptations, one of the most interesting underwater animal imaging system belongs to the mantis shrimp [28]. This animal, a denizen of clear tropical waters, possesses a multitude of spectrally sensitive photoreceptors, with several of the absorption pigments in the ultraviolet [29]. The use of such a spectrally resolved system is thought to play an important part in intraspecies communication and in the recognition of individuals.

Polarization is another adaptation that can be found in a multitude of underwater animals. This includes the mantis shrimp as well as octopus and some fish [30]. The use of polarized vision in underwater animals has been discussed as a navigational aid [31], enhanced vision in the presence of backscatter [32], enhanced detection of semitransparent prey [33] as well as a means of communication [34].

### *B. Early Imagers*

As described [3], the first believable report of human underwater imaging was due to Konrad Kyeser, who in 1405 entered the water in his leather suit with flat glass plates to see through into the water. However, as legend has it, Alexander the Great was very interested in seeing underwater. As time went on, a conjecture that he actually had been underwater took hold and many manuscripts documented this historically imagined event. Fig. 6, reproduced from a German manuscript from ∼1405, shows Alexander underwater in a glass diving bell with a dog, a cat, and a rooster. The legend recounts that his wife and her lover then cut the chain that was his connection to the surface, leaving him to his own devices to figure out how to escape back to land. Remarkably, he did. Fascination with underwater imaging was clearly present in the middle ages.

On a somewhat more contemporary note, in the 19th century, there was great fascination in exploring the ocean, somewhat akin to our 20th century fascination with space. As such, submersibles were built to carry humans into the shallow depths. Many of these had underwater viewing ports that allowed seeing into perhaps the murky harbors that the submersibles were deployed in. Two interesting examples were the German built submersible "Sea Devil," built in 1856, and the Ictineo I and II, designed and built by the Catalan designer Narcis Monturial in 1861 and 1864. The Sea Devil is credited with taking the first underwater picture, a foggy image of some rocks. Fig. 7 shows a replication of the Ictineo (length equal to 7 m). The ports for viewing are clearly visible in the front, bow, top, and sides.

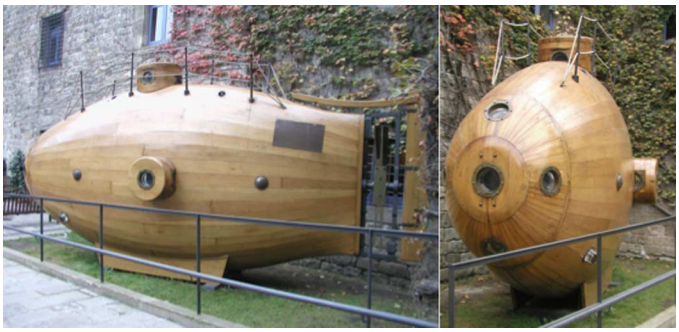

Fig. 7. Photograph of the replication of the Ictineo I, located at the Marine Museum in Barcelona. (Courtesy Jaffe, 2002.)

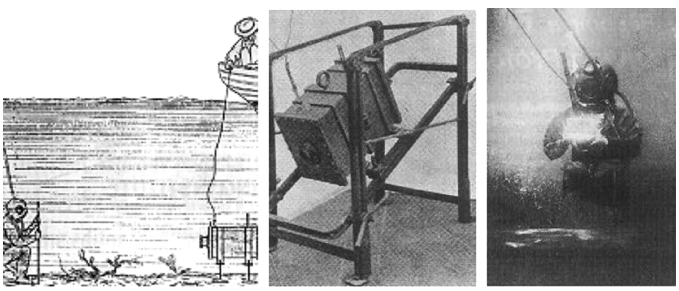

(a) (b) (c)

Fig. 8. (a) Schematic of Louis Boutan's underwater camera system. (b) The underwater camera. (c) Photo of a hard-hat diver at work (1893).

The next great advance in underwater imaging accompanied the advent of diving suits. One of the earliest pictures, although there seems to be some debate [3], was taken by Louis Boutan who took pictures of either himself or a fellow diver in 1893 at the French Mediterranean coast at a depth of more than 50 m. Fig. 8 shows the setup, camera, and one of the pictures taken. As reported, the development of arc lamps and then a magnesium powder flash facilitated shorter exposures and allowed Boutan to not have to stand still for 30 min underwater. In this case, photosensitive glass plates were used to record the images.

### C. Imaging With Film

Two major advances in the 20th century facilitated the proliferation of underwater imaging: 1) the development of the film camera, starting in the 1890s with George Eastman; and 2) the development of the Aqua-Lung in the 1940s by Cousteau and Gagnan. The first underwater color pictures were reported to have been taken in 1926–1927 by William Longley and Charles Martin off the Florida Keys.

As reported in [3], "Bruce Mozert developed still and video housings and underwater flash systems in the 1930s. Haas developed the popular 'Rolleimarin' camera in 1943; and in 1957 Cousteau conceived the Calypso camera that in 1961 went on to become the best known underwater camera of the 20th century as the 'Nikonos'."

Moving ahead, the next major advances, motivated by the quest for scientific exploration, took place in the 1970s, when, in a geological context, several deep towed camera systems were developed. At the Scripps Institution of Oceanography (La Jolla, CA, USA), Fred Spiess' group developed "Deep Tow" [35]. A famous example of its use was in the 1976 survey of the Galapagos rift that detected temperature anomalies, presumably due to hot springs. A somewhat different system, ANGUS, built at the Woods Hole Oceanographic Institution (WHOI, Woods Hole, MA, USA) by Robert Ballard and associates, consisted of a towed camera sled that was lowered to a depth of 6100 m. It was used in the Galapagos Hydrothermal Expedition in 1977 and, as reported [36], resulted in spectacular images of fields of deep-sea clams. The images were the first indications of the unique and astounding biological environments that were located at the sites of these underwater geothermal fields or hot vents. Subsequent investigation revealed a unique ecosystem that was not dependent on photosynthesis but rather "chemosynthesis." Heralded as one of the most important discoveries of the 20th century, it was the result of undersea exploration using underwater optical imaging [37].

### D. Modern Age for Underwater Optical Imaging: Electronic Imaging

Although the film camera opened up a new revolution in underwater photography, an area that was still badly in need of technical advance was the capability to view underwater images, taken from a remote platform, from a surface vessel. To achieve this goal, Ballard's group at WHOI developed the ARGO system [Fig. 9(a)] [38], a substantial advance for deep-sea underwater imaging. The system consisted of a towed sled, much like the acoustically navigated geological underwater survey (ANGUS), but in addition to the film cameras the vehicle was equipped with video cameras that permitted real-time viewing via a cable. The most famous image produced by ARGO, shown in Fig. 9(b), was a picture of one of the giant boilers from the sunken luxury liner Titanic, confirming that the hull was nearby. The real-time data proved indispensible in making adaptive decisions about seafloor mapping strategy.

Subsequent developments in underwater optical imaging progressed as the revolution in digital recording, transmission, and data processing continued. As seen in Fig. 9(b), the degraded, fuzzy image was just interpretable, however, in need of vast improvement. The subsequent use of digital cameras with high dynamic range provided a great advance in underwater imaging in that the backscatter from the reflection of the near-field light could be ameliorated by contrast equalization of the images.

Last, we present a note about the history of the study of the physics of underwater image formation and its use in optimizing the configuration of underwater optical imaging system performance. During the 1960s, a center of excellence in underwater optical imaging was first established at the Massachusetts Institute of Technology (MIT, Cambridge, MA, USA) and then moved to the Scripps Institution of Oceanography. Under the direction of S. Q. Duntley, the lab spent several decades both refining the limits of, and working on new technology to improve underwater imaging until it was disbanded in the 1980s. Duntley's seminal paper "Light in the sea" [39], published in 1962, highlights the fact that "the long research program, spanning two decades," on underwater optical imaging by the U.S. Government actually started during World War II. At the same time, largely unbeknownst to the west, work in the former Union of Soviet Socialist Republics (U.S.S.R.) progressed mostly on a


(a) (b)

Fig. 9. (a) ARGO video sled. (b) Image of one of the boilers of the sunken luxury liner Titanic, taken in 1985 (Woods Hole Photo Credit).

theoretical basis, however, with some experimental work. Many references to work in radiative transfer as well as the theory of optical imaging in scattering media are referenced by Zege *et al.* in [40]. A third center of excellence was established in Denmark, largely through the work of Jerlov [1], [13] and colleagues.

## IV. Underwater Systems: Principles and Design

As a general classification, considered above, underwater imaging systems can be regarded as either "passive" or "active," the difference being whether the imager creates the light (active) or not (passive). Although these two systems are different, the properties of the light field and how it is transformed during propagation unifies them and, moreover, provides a common context for understanding underwater optical imaging.

Visibility is an important concept in imaging that can be the ultimate consideration. As such, it has been treated in detail in many contexts. As one measure, contrast defines the relative difference between adjacent areas as a function of the SNR. The psychophysics of human vision continues to be an interesting area of research that yields information about perception that will not be discussed here, other than to say that it is often fascinating to see how human vision and perception can often discern patterns in images that are seemingly difficult to quantify.

### *A. Passive Optical Imaging*

Notably, the first case of obtaining a quantitative estimate for the clarity of imaging underwater was obtained from the measurement of the visibility of the Secchi disk. Created by Angelo Secchi in 1865, the disk consists of the black and white pattern, shown in Fig. 10, printed on a circular disk. The distance where the disk vanishes, as seen by a human observer, is taken as the measure of the water's transparency and referred to as the Secchi depth. Thus, a human observer who noted visibility performed the first quantitative measure of water clarity. Before the advent of inexpensive optical meters to measure the IOPs, Secchi disks were used to characterize the opacity of the water [41]. The measurement of Secchi disk visibility and its correlation with the inherent optical property "$c$" is remarkably robust.

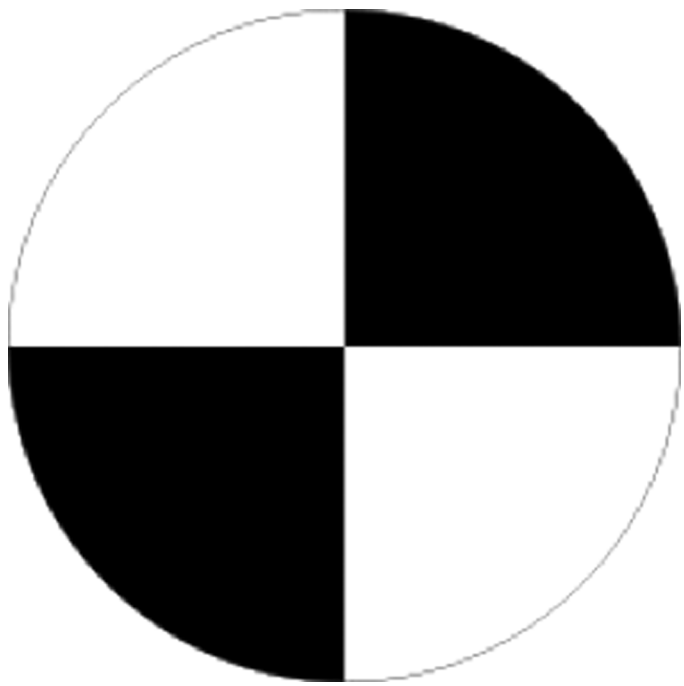

Fig. 10. Secchi disk pattern.

This measurement (in meters) divided into 1.7 yields the attenuation coefficient "$c$" averaged over the depth where the disk vanishes [42].

Imaging underwater using ambient sunlight as the light source is the only option for the vast majority of biological underwater imagers. In clear sunlit water, the visibility of many objects is good and, hence, prey are in danger of being discovered by their predators. Hence, crepuscular periods are chosen to forage. Underwater visibility in ambient light has been of long-standing interest. The visibility of an object in ambient light was considered by Duntley [39]. Here, decades of underwater visibility experiments were summarized by stating: "Along an underwater path of sight a remarkable proportion of the objects ordinarily encountered can be seen at limiting ranges between 4 and 5 times the distance $1/[c - K(\theta, \varphi, z)\cos(\theta)]$, regardless of their size or the background against which they

appear." Here, $K(\theta, \varphi, z)$ is the diffuse attenuation coefficient, an apparent optical parameter (AOP).

The contrast of a black target viewed horizontally in a sunlit ocean was considered in [43] where the simple parameter $y = 4.5/c$ ($c$ being total attenuation in $\mathrm{m}^{-1}$) was found to be a good approximation for maximum viewing distance. Note that the contrast measure for this threshold was defined as the fractional contrast in radiance of the target $(T)$ to the background $(B)$

$$C_v = \frac{L_T(\theta, \varphi, z) - L_B(\theta, \varphi, z)}{L_B(\theta, \varphi, z)}$$

where the success of the imaging system is judged by the ratio

$$\frac{C_{vr}(\theta, \varphi, z)}{C_{v0}(\theta, \varphi, z_T)} = \exp[-cr + K_B(\theta, \varphi, z) r \cos\theta]$$

as set by Duntley, to exceed a value set as a parameterization of human vision [44]. We also note that there is some simplification here as the visibility range is also a function of the target's detail. In practice, regarding human detection, an additional consideration is the wavelength dependence. For humans, this would be under scotopic (low-light) vision, where the retinal rods are sensitive, or photopic (high-light) vision, where the retinal cones are performing the sensing.

As previously discussed, the concept of contrast was used by Nilsson *et al.* [26] where the ability of the giant squid eye to image at depths of 500–1000 m was investigated. The question was why squid have such large eyes when, in fact, the ambient light levels are too low to confer an advantage in using ambient light for imaging. The solution, the authors suggest, is that squid are adapted to see the bioluminescent clouds that are excited by the swimming of their large predator, the sperm whale. Although the details of the analysis are somewhat beyond the scope of this paper, we note that the contrast value that was used followed the arguments in [25]. Here, a Gaussian distribution of photons is assumed and the discrimination between the signals in two channels is possible when the difference is greater than or equal to a reliability constant $R$ times the standard deviation of the difference (which is the square root of the sum of the two means). So that

$$\frac{|N_T - N_B|}{\sqrt{N_T + N_B}} \geq R$$

where $R = 1.96$ for a 95% confidence level and $N_T$ and $N_B$ are the number of photons in the target and the background. Note that, as considered here, contrast is a function of background to target difference, as above, however, now divided by the square root of the sum as it takes into account the Gaussian nature of the image noise.

The potential facilitation of underwater visibility by the use of polarization has fascinated underwater imaging researchers for some time. The possibility exists as the ambient light field is polarized and the use of polarization may provide contrast between the dichroic behaviors of objects of interest that will reflect light with the ambient field. As considered above, many animals have the ability to detect polarized light. This ability might be used to facilitate the detection of conspecifics via signaling [45] or, to increase imaging ability to perceive objects [46].

From a historical perspective, early investigation of ambient polarization and its potential use in producing higher contrast images with polarizing filters was due to Waterman [47] with further work in [30]. More recently, a number of studies by Schechner and colleagues demonstrated that taking several underwater pictures with different polarization settings could be used to improve the images and also provide a distance range [48]. A recent review is contained in [49]. However, the use of polarizing filters always results in a decrease in received light and, therefore, the statistics of the increase in contrast as a function of polarization must provide an overall gain in contrast, even in the presence of a decrease in light values measured.

An important aspect in modeling underwater ambient imaging is to estimate ambient light levels. As considered, the state variable for underwater light is radiance, and the equation that governs the propagation of light is the radiative transfer equation. This equation governs the dynamics of energy transformation in a great many physical situations [50]. In the situation considered here, the input to the equation is the incident sunlight on the sea surface, its penetration through the air–water interface, and the water properties that govern the transformation of this light via absorption, scatter, and some of the inelastic processes such as fluorescence and Raman scatter. The classic work on underwater radiance is the book series by Preisendorfer [51]. A modern popular reference is [10]. Solving the radiative transfer equation with sunlight as the input will yield the underwater radiance as a function of location. This has been considered for many years now, however, a general theoretical solution for spatially varying IOPs is difficult, if not impossible, without extensive computational power.

A pragmatic solution to predict underwater radiance is the Hydrolight Model [52]. The model uses the invariant embedding technique [10] and can accommodate depth-varying IOPs while providing output such as the radiance and a variety of AOPs such as the diffuse attenuation coefficient. Validation has occurred in a number of circumstances [53]–[55]. The model is commercially available (Sequoia Systems, Bellvue WA). As configured it does not include polarization.

### B. Active Optical Imaging

As defined, the use of artificial illumination for underwater viewing is referred to as "active." There is great interest in active underwater imaging as an improvement in image quality can be obtained when the illumination is controlled and coordinated with the receiver. In this context, the job of the underwater optical imaging system designer is to optimize the performance of the system via the hardware configuration of the components. To aid in this process, computer modeling of underwater image formation can provide a basis for system design. Accordingly, a number of approaches can be taken. The most exact is to solve the radiative transfer equation. However, this can be quite difficult and may not provide a great deal more insight than simpler methods that use either ray trace or Monte Carlo methods that follow single photons that eventually lead to image formation. Computer processing typically follows such designs and may be an integral part of the imaging as in the case of computational imaging [56].

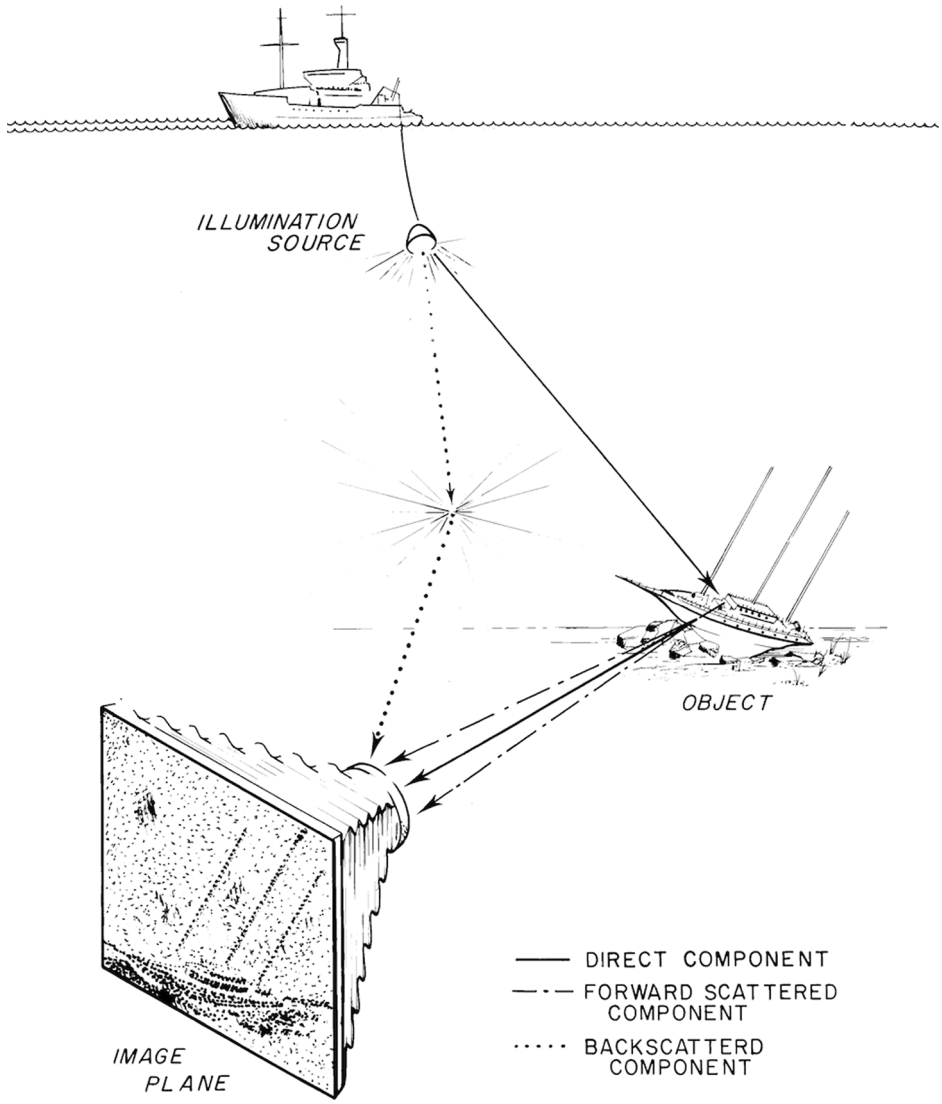


Fig. 11. Three imaging components and three hardware components in the UNCLES underwater imaging system [57].

Here, the geometric approach embodied in [57] is considered in some detail as it leads to an understanding of the basics of the underwater image formation process via a relatively simple formulation. Fig. 11 illustrates that an underwater imaging system is considered to consist of three components: lights, cameras, and the intervening water. The images formed are then regarded as consisting of 1) a backscatter or volume scatter component of light that has not interacted with the target; 2) a "direct" component of light reflected from the target that has not been scattered on its way back to a camera; and 3) a "blur" component that consists of light that has been reflected from the target that is then scattered on its way back to the camera. An additional feature of this model, not shown in the figure, is that the light is also blurred as it transits from the source to the target.

Considering first the backscatter component, the model uses ray optics to determine the irradiance in watts per squared meter (after total attenuation) incident on the volume that the camera is viewing. Using spatial discretization, the VSF is then used as a weighting function to determine the magnitude of light that is backscattered to the camera by considering the angle between the incident and reflected light. Next, given the light incident on the target (after attenuation), a reflectance map $\rho(x, y)$ is used to compute the reflected light. The reflectance map is considered to be a function of the position $(x, y)$, the incident $(\theta, \varphi)$, and reflected angles $(\theta', \varphi')$, as is standard in computer graphics [58]. The function is usually parameterized to that

$$\rho(x, y, \theta, \varphi, \theta', \varphi') = \rho(x, y)\ \mathrm{BRDF}(x, y, \theta, \varphi, \theta', \varphi')$$

where BRDF is the bidirectional reflectance directivity function. Here, a simple Lambertian model for the BRDF is used, however, note that a set of BRDFs for the sea bottom in a tropical environment were measured [59]. Using this function and the irradiance of the incident light field on the target $E_t(x, y)$, the "direct" component can be computed from ray optics, as described in [57].

A natural consequence of transmitting an image through a scattering medium is that the image is blurred. A simple, and often used, approximation is that the resultant image is the convolution of the image that would have been obtained in the absence of the scattering media with a kernel function. This kernel,

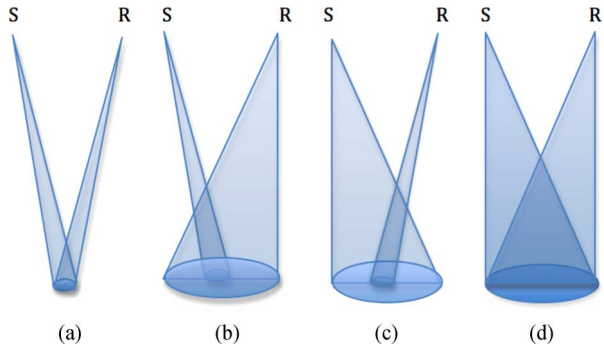


Fig. 12. Categorization of imaging system types: (a) narrow-source–narrow-receiver system; (b) narrow-source–wide-receiver system; (c) wide-source–narrow-receiver system; and (d) wide-source–wide-receiver system (modeled after [40]).

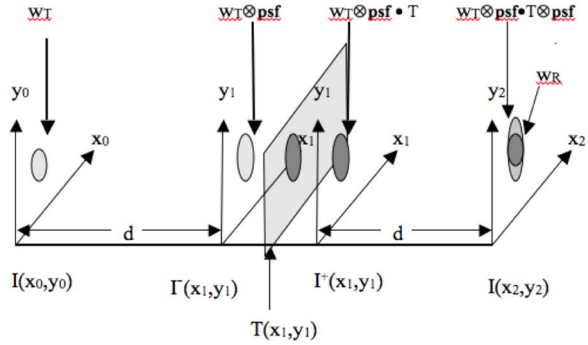


Fig. 13. Illustration of the geometry of the approach taken in estimating the performance of the systems shown in Fig. 12.

equivalent to the point spread function (PSF) [60] is a function of both the IOPs and range. The range dependence is explicit as images become more blurred when viewed from farther distances due to the increased amount of scatter.

As one example [57], the formulation considered in [61] was used to compute an image that uses the expression

$$E(x,y) = E_b(x,y) \otimes \{\exp(-Gr) - (cr)\} F^{-1}[\exp(-Brf)]\}. \tag{4}$$

Here $E_b(x,y)$ is the blur component, $r$ is the range from the target to the receiver, and $\otimes$ is the convolution operator. $G$ is an empirical constant ($|G| \leq c$) and $F^{-1}$ indicates that an inverse Fourier transform is taken of a function that contains $B$, an empirical damping factor, and $f$, a radial frequency in cycles per radian. The form of the PSF and its relationship to the small angle scatter of the VSF has been studied in great detail [62], [40]. An additional aspect of (4) is the range of its validity. Since the overall PSF (all other terms are weighting) can be defined as $H$, then

$$\begin{aligned} H(B, r_1, r_2, f) &= F^{-1}[\exp(-B(r_1 + r_2)f] \\ &= F^{-1}[\exp(-B(r_1)f)\exp(-B(r_2)f)]. \end{aligned}$$

This implies that

$$H(B, r_1, r_2, f) = F^{-1}[\exp(-B(r_1)f)] \otimes F^{-1}[\exp(-B(r_2)f)].$$

So that the overall PSF can be viewed as

$$H(B, r_1, r_2, f) = H(B, r_1, f) \otimes H(B, r_2, f).$$

A consequence of this is that, at twice the range, the total PSF is equal to its autoconvolution. To determine the ranges at which this treatment is valid, a comparison of the linear theory with the predictions of a Monte Carlo model was performed [63]. Here, it was shown that this simplified treatment differed from the Monte Carlo results for the lowest frequencies in the Fourier transform of the PSF, however, was valid at the highest spatial frequencies out to ten attenuation lengths, the longest distance considered.

To better understand the advantages and limitations of various configurations of underwater imaging systems, a basic classification was formulated [40]. As illustrated in Fig. 12, four systems are shown that have various source/receiver configurations. Note that the source and receiver patterns shown are for a single transmit or receive element that scans a target on a point-by-point basis to form an image. In the system shown in Fig. 12(a), the source provides a narrow illumination, while the receiver integrates over a narrow field of view. In the system shown in Fig. 12(b), the source illuminates a narrow field of view, while the receiver integrates over a wide one. In the system shown in Fig. 12(c), the roles are reversed. In the system shown in Fig. 12(d), a wide source and a wide field of view lead to no image capability at all.

As described [64], in the absence of backscatter, the image $I(x', y')$ resulting from these systems can be determined by

$$\begin{aligned} &I(x', y') \\ &= \iiint w_R(x_2, y_2) w_T(x_0, y_0) \mathrm{psf}(x_2 - x_1, y_2 - y_1 : d) \\ &\quad \times \mathrm{psf}(x_1 - x_0, y_1 - y_0 : d) T(x_1 - x', y_1 - y') \\ &\quad \ldots dx_0 dy_0 dx_1 dy_1 dx_2 dy_2. \end{aligned}$$

The geometric interpretation of this equation is shown in Fig. 13, where starting on the left, the figure shows the projection of the source onto the plane $(x_0, y_0)$ resulting in the light field $I(x_0, y_0) = w_T$, the weighting function of the transmitter. This irradiance is then propagated to the right to just before plane $(x_1, y_1)$ to obtain $I^-(x_1, y_1)$ by convolving this with the PSF of the medium. The light is then attenuated by the screen $T(x_1, y_1)$ via multiplication to yield light distribution $I^+(x_1, y_1)$. Propagation to the plane $(x_2, y_2)$ occurs via convolution with the PSF to yield light distribution $I(x_2, y_2)$. This light field is then integrated over the region shown as $w_R$ (the small circle inside the ellipse), the weighting function of the receiver, to yield a single value for the image that is formed. An image can be formed by translating the attenuating screen by $(-x', -y')$: $T(x_1 - x', y_1 - x')$ to obtain each value in the final image $I(x', y')$.

If both weighting functions are delta functions, somewhat similar to a laser line scan system, the equation yields an overall PSF that is the product of the two medium PSFs. This results

in the best resolution possible as the product reduces the sidelobes relative to the peak value. If either the $W_T$ or $W_R$ functions are constant, i.e., encompass a large field of view, as in Fig. 12(b) and (c), the system resolution degrades to that of the one-way PSF. In the fourth case, only a very poor image is possible, as the wide patterns of illumination and reception lead to substantial blurring. Interestingly, a similar formulation emerges in the case of confocal optical imaging [65], where the source and receiver PSFs combine as a product to increase system resolution in the exactly the same way.

Armed with the realization that a narrow source and a receiver produce the best resolution of these configurations, there have been several "advanced" systems that have attempted to get as close to case 1 as possible. The LBath system [66] utilized a narrow scanning beam with a staring array, a 1-D CCD. As each element of the CCD array has a small angle of acceptance, and the transmit beam is narrow, the system approximates the geometry of Fig. 12(a). An additional benefit of the LBath system is that it can judge range via the use of triangulation.

The Laser Line Scan System, a commercial system manufactured by Raytheon in the 1990s provided excellent images in many situations [4]. The system scanned a narrow beam from side to side and recorded the reflected light through a narrow slit that was synchronously scanned via a rotating shaft with faceted mirrors. Several versions were produced, the most sophisticated being a four-channel version that was used for fluorescence imaging of corals, permitting some degree of taxonomic discrimination [67]. A well-known expedition deployed the system from the Johnson Sea Link to image the MONITOR Civil War wreck [68].

More sophisticated schemes for projecting light beams can also be utilized as in [69] where projection of an array of beams, over the field of view of a narrow, staring array, was proposed. This geometric arrangement can be considered to be a parallel implementation of the above, single scanning beam, the basic idea being that, as long as the beams are spaced far enough apart, the individual, projected elements can be considered to be independent. Therefore, a superposition of such beams results in an image like that produced by the system depicted in Fig. 12(a).

An interesting variant on underwater imaging accomplished in the SIO Visibility Lab in the 1960s was the TVI system. The system, declassified in the early 1990s [70], uses an extremely small source held very close to the target to approximate, as close as possible, a self-illuminated target. In the limit that the incident light becomes a delta function, the image formation process approaches the geometry in Fig. 12(b) and the resultant image becomes

$$I(x',y') = \iiint w_R(x_2,y_2)\mathrm{psf}(x_2-x_1, y_2-y_1 : d) \times T(x'-x_1', y'-y_1')dx_1dy_1dx_2dy_2.$$

Note here that since only a small portion of the target is "lit up," the reflected information is only a function of that small area, leading to excellent images in high scatter. In the original publication, a small, scanning, laser illuminator was used that was held close to the target and synchronized to a surface receiver by the emission of a light pulse of a different wavelength. The original motivation for the system's performance specification was to allow a portable, diver deployed illuminator to be the only "in water" component. Note that the overall PSF for the system is now due only to the spreading of the illumination beam on the way from the source to the reflectance map. Therefore, illuminating the target from very close range will minimize spreading of this PSF and result in a sharp image.

A modern enhancement of the system was considered in [71]. Here, the investigators replaced the synchronization pulse with a modulated laser. This permitted the start and end of each line to be recognized without the use of a separate synchronization pulse. The improvement highlights that the system is really a "free space" optical telemetry system, where information about the image has been encoded into the 1-D light propagating in the water. Images taken with the system are quite impressive. If the water is entirely scatter dominated, very large numbers of attenuation lengths ($\sim$70) are achieved, only a function of the ability to collect the scattered light. However, real water has a substantial amount of absorption that needs to be incorporated into the lab results to obtain realistic values for range.

### C. Pulsed Systems for Underwater Imaging

As above, an additional degree of freedom in constructing underwater optical imaging systems is to either pulse or modulate the light source. In the simple case that the light source is a short pulse, the system is called LIght Detection And Ranging (LIDAR) or LAser Detection And Ranging (LADAR). Examples of LIDAR used in atmospheric optical systems abound. One such system for looking into the ocean from an airborne platform is described in [72]. Imaging through a time varying 3-D modulated sea state is challenging for obtaining high resolution. The system described in [72] has, therefore, been used mostly for detection of fish and plankton, although spatial maps of the depth dependent reflectivity have generated interesting environmental measurements.

A significant advantage of LIDAR systems is that they "gate out" the near-field backscatter that can overwhelm the sensor. The receiving element, typically a photomultiplier tube (PMT), must therefore be switched off and then on in rapid sequence with the occurrence of the end of a previous pulse (off) and the start of the imaging volume, judiciously chosen to eliminate the near-field backscatter (on). This has created a significant, but not insurmountable, challenge to the underwater imaging community where the distances between the on/off gating are much shorter than that of the airborne LIDARs.

In addition to gating out the near-field backscatter, another advantage of LIDAR systems is that the round-trip transit time of the pulse can be estimated. This then permits an estimate of the range of the target. Since light travels approximately 22.5 cm/ns in seawater, nanosecond pulses are needed for a range accuracy of tens of centimeters in the cloudiest waters. Techniques for achieving superior range resolution to this require either clear water, where interpolation can be accomplished, or more advanced detection and, perhaps, modulation schemes, to be considered in Section IV-D.

A system that propagates a short pulse of light into the 2-D field of view and then gates the receive pulse to eliminate the near-field backscatter is the LUCIE System developed by

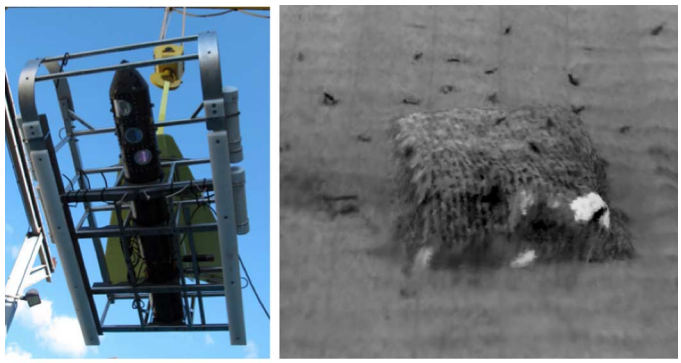

(a) (b)

Fig. 14. (a) $L^2S$ system under development by Jaffe [76]. Shown is a tow sled and a cylinder that houses the system. (b) A rendered image of the point cloud and reflectance map that was generated from the collected data showing a discarded lobster trap at 70-m depth in waters close to San Diego, CA, USA.

Fournier *et al.* [73]. The system employs a standard Nd:YV04 20-kHz diode-pumped laser at 532 nm with 600 mJ of power to illuminate a 45° or 15° field of view. A variable range gate from 3 ns with 100-ps increments is used to record the reflected light. Eliminating the backscatter leads to increased SNR and longer viewing ranges, depending on the IOPs of the water. A commercial version of the LUCIE3 system is being marketed (Neptec Technologies Corp., Kanata, ON, Canada)

One active imaging system that has seen extensive deployment is the Streak Tube Imaging Lidar (STIL) by Arete' Associates (Arlington, VA, USA). The system works by projecting a short pulsed sheet of light that is then temporally and cross-track spatially displayed as a 2-D image in a streak tube. The image is recorded and processed to yield cross-track range and reflectivity [74]. A more recent extension and development of the system is the multislit STIL (MS–STIL) [75] that enables simultaneous detection of multiple spatial–temporal channels. The channels have been used in a variety of ways to generate images such as single-pulse 3-D "flash" LIDAR images, 3-D multispectral images, and 3-D polarimetric images.

As one example of a multilook LIDAR system that uses scanning beams, the Laser Lidar System ($L^2S$), recently developed by Jaffe [76] surveys a 70° swath of sea bottom at a scan rate of 160 lines/s by propagating a 3.5-ns laser pulse that is transmitted with a 1-MHz repetition rate to achieve a cross pixel output of close to 4000 values. Estimation of both the target range and reflectivity, as described above, permits the production of 3-D reflectance maps. Although a complete description of the system awaits a future publication, a recent sea trip yielded some impressive images, one of which is shown in Fig. 14(b) along with the system, mounted on a tow sled, in Fig. 14(a).

### D. Temporally Modulated Light

In pursuit of ever more imaging system performance, the use of advanced techniques continues, largely driven by the great contemporary advances in the electro–optics commercial marketplace. For the most part, the degrees of freedom available to the underwater imaging engineer are limited to changing the spatial and temporal characteristics of the light source in conjunction with the receiver.

In the case of temporally modulated waveforms, the initial work of Mullen *et al.* was geared toward improving the imaging capability of the Raytheon Laser Line Scan System discussed above [77]. Desired outcomes of the advanced system were less sensitive to solar radiation, and a decrease in the near field, backscatter component. As documented, the authors imposed a 10-, 50-, or 90-MHz modulated envelope on the transmitted light that was then postprocessed after receipt to remove the "out of band" frequencies, presumably induced by the washed out response of the backscatter. The relative phase of the backscattered signal also provided range information (modulo phase/$2\pi$).

The modulated laser idea was extensively modeled [78], and more recent work at high modulation frequencies (100 MHz–1 GHz) to decrease the forward scattered or "blur component" has been accomplished. Further work by this group is contained in [79] where work is described to evaluate the capability of higher modulation frequencies to decrease forward scatter.

### E. In Situ Macroscopy and Microscopy

In this section, underwater optical imaging of objects in the tens of centimeters to micrometer range is considered. Although the intent is to highlight seagoing systems, some lab systems are described that have potential to transition to at-sea deployments. A somewhat subjective boundary of 30–100-$\mu$m resolution is defined to discern the difference between macroscopy and microscopy. This is a convenient break point, as a large number of systems have been developed for water column imaging of zooplankton that are macroscopes, while there are relatively few *in situ* microscopes. In both cases, since the viewing distances are relatively short with respect to the absorption and scattering lengths in most open oceanic conditions, the limitations due to these effects are ameliorated. The imaging systems have been applied to characterize both suspended and bottom dwelling organisms and particles in the sea.

*1) Underwater Macroscopy:* In the case of *in situ* macroscopy, it is likely that the first such system was the shadow graph system developed by Ortner *et al.* as a silhouette system to take pictures of plankton [80], [81]. The fundamentals of silhouette photography are described in [82] where it is demonstrated that a highly collimated beam of light imaged with a high $f$-number camera facilitates a large depth of field. This is useful for keeping subjects in focus over a large volume. Since the pioneering work of Ortner *et al.*, a number of systems have been developed to image a variety of macroscopic pelagic species [83]. Most of these systems employ some variant of the shadow graph or another method known as dark field illumination that projects a conical, or off axis beam, at the specimens so that only scattered light is imaged. This has great advantage for translucent organisms such as many of the plankton in increasing contrast.

Underwater holographic imaging systems have continued to develop since the pioneering work of Carder [84], [85] and the group of Acosta at collaborators at the California Institute of Technology (Pasadena, CA, USA) [86]. Over the last decade a number of these systems have progress rapidly as the transition from film to digital imaging facilitated both recording

and processing [87], [88]. A holographic imaging system, the LISST-Holo, is currently being marketed by Sequoia Systems (Bellvue, WA, USA) that is based on a design by Graham and Nimmo-Smith [89]. Holographic systems have a great advantage in that the depth of field is quite large, especially compared with a conventional camera system that trades resolution for depth of field.

Although there are now both seagoing conventional (shadow-graph-dark field) and holographic systems, the shadow-graph systems seem to have more popularity for survey as evidenced by their proliferation and the large literature that their use has generated. This may be because the data are easier to interpret and/or the systems are easier to fabricate. However, one large disadvantage of these systems is that it is difficult to measure organism abundance because, due to the depth-dependent defocus, the detection volume for small to large organisms changes as a function of size. Since the holographic systems can estimate 3-D positions, their ability to estimate density is better than that of the simple shadow graphs. Stereo macroscopy does not suffer from such limitations [90], however, images smaller volumes than holograms.

In considering images that are produced from both the conventional and holographic imaging systems, the overwhelming need is to now develop automated recognition algorithms. There has been some excellent progress in this area [91], however, the remaining taxonomic discrimination that is necessary for a more complete characterization of the ecosystem beckons [92].

As another example of a macroscopic technique, the use of planar laser imaging fluorometry (PLIF), as described in [93] and [94], has demonstrated results in characterizing fluorescent particles in the water column. The technique, originally demonstrated in the lab [95], [96], was then used at sea on the free-fall imaging device for oceanography (FIDO) free-decent vehicle. More recently, the data obtained from the system indicated the presence of "cryptic peaks" of larger fluorescent particles that were undetected in the bulk fluorescence measurements [97], [98] further confirming that the vertical structure of the ocean is, indeed, quite different at meter scales throughout the photic zone. The system has roughly 100-$\mu$m resolution, however, it is capable of detecting fluorescence from individual phytoplankton as small as 20–30 $\mu$m [99].

*2) Underwater Microscopy:* Underwater microcopy, as defined above, is related to systems that collect images whose resolution is substantially better than 30 $\mu$m. Such systems naturally have a small field of view, however, due to the prevalence of microorganisms in the global ecosystem, their characterization is important [100]. In addition, the continued and increasing prevalence of harmful algal blooms [101] and their early detection renders this an attractive area for continued technical development.

As one variant on an underwater microscope, there are several flow-through systems that can be deployed *in situ*. The systems pump small organisms through a microfluidic chamber to guarantee that their subjects will be imaged inside the limited depth of focus that occurs at these high magnifications. Two prominent systems are the Flow Cytobot [102] and the commercially available FlowCam (Fluid Imaging Technologies, Scarborough, ME, USA). In the case of FlowCytobot, a set of image processing and identification algorithms have aided in automatic identification [103].

In addition to systems that look at microscopic life that pump water through a flow chamber, systems that can also peer into the water through a port have been developed. One system with demonstrated success is the holographic microscope developed by Sheng *et al.* [104], [105] who, over the last decades, have displayed the usefulness of such systems, mainly in the lab, for deciphering many interactions on these microscales. A recent demonstration of a seagoing version of the system [106] showed, among other results, that diatom chains were preferentially horizontally oriented in the direction of flow, indicating a shear. A holographic microscope for *in situ* studies is being marketed by Resolution Optics (Halifax, NS, Canada). Other work, by other prominent groups in this area, is described in [107] and [108]. Note also that since the resolution obtained in a holographic imaging system is mostly a function of the system's capability to collect scattered light, the holographic systems described previously are capable of this higher resolution.

A somewhat unexplored option, the use of long working distance lenses with LED illumination in a more conventional geometry, has been under development by this author and coworkers for several years now [109]. Although these systems suffer from a short depth of field, the large natural abundance of small particles such as protists permit obtaining many interesting images. As with shadow-graph systems, volumetric estimation of abundance is difficult to obtain without using stereographic methods or some other means for either localizing the target or calibration. Nevertheless, the data are straightforward to obtain and permit the use of various incoherent image modalities that have proved to be quite useful in conventional, land-based, microscopy. Several pictures from a seagoing version of the system [110] are shown in Fig. 15.

### *F. Prospects for Improved Performance*

*1) Coherent Imaging:* Among the various techniques for imaging through a scattering medium, coherent techniques have been shown to offer advantages, especially in biomedical imaging where optical coherence tomography (OCT) has become a standard method for viewing various classes of objects. The central idea with OCT is that signal enhancement will result from processing a complex waveform that is propagated into the medium and then detected using heterodyne techniques. In the case of a temporally coded waveform that is reflected from a "hard target," the photons that have not been scattered on the way back to the receiver will return with the identical temporal code, allowing a matched correlator to have good success. In the case of coherent imaging, since the waveform is both amplitude and phase encoded, higher discrimination can be had, as the phase coding is subwavelength and, therefore, of higher resolution. On the other hand, if the medium is fluctuating and interposing various temporally varying objects with different refractive indices, the processing gain of a coherent system will be limited. Although underwater imagers could potentially use coherent imaging methods, there has been relatively little published work in this area. Data of interest, for example,

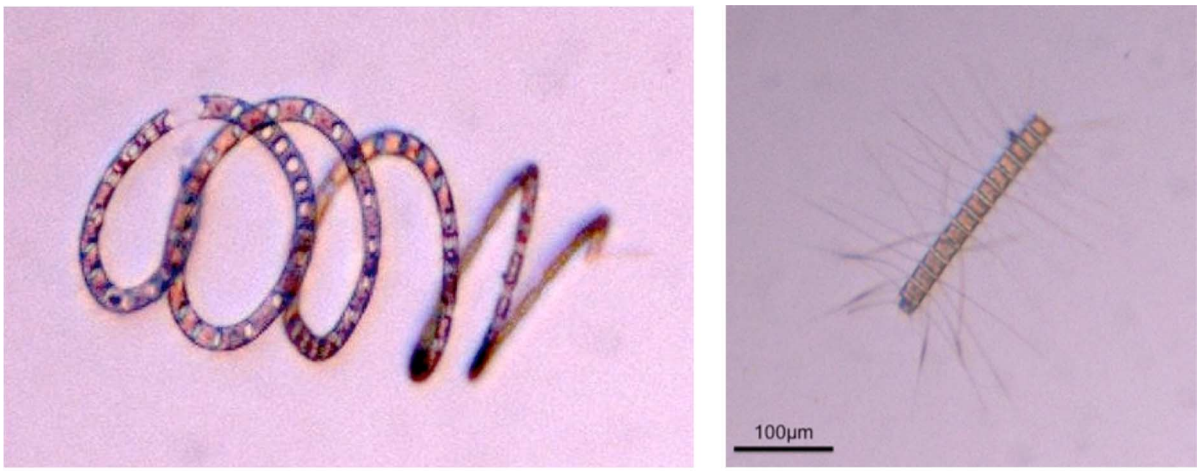


(a) (b)

Fig. 15. Several images of phytoplankton collected at sea with an underwater microscope system [105]. (a) Helical spiral of Eucampia cells, a diatom. (b) Linear chain of the diatom type Chaetoceros

would be the decorrelation time of the ocean in a variety of environments.

In one of the earliest examples of coherent imaging through a scattering environment, Stetson [110] imaged a pitcher in a small tank filled with water with suspended particles. Although no pictures were shown or analyzed quantitatively, the author claimed that via simple viewing, the use of coherent methods yielded better images than those that did not. In other work, to measure the spatial distances over which light can propagate and still remain coherent, Stachnik [111] summarily stated that "coherent behavior is observable in coastal Atlantic waters at a range of 7.84 m (4 attenuation lengths) and that the interference patterns that form have good linearity, but can vary significantly in contrast."

Considering much later work, Caimi *et al.* [112] concluded that preserving the phase of an underwater optical signal was subject to great variability and strongly dependent on effects such as turbulence. As they state in their paper, "generally, the demands of maintaining a spatially coherent beam at optical frequencies is difficult over long range thereby limiting the usefulness of the technique for image formation in turbid media." Given the success of the holographic techniques, as summarized above, the use of coherent imaging over paths as short as a few centimeters indicates that, over these very small distances, coherent scatter from suspended targets is preserved. Maximal distances for such methods to work in extending underwater optical imaging are, therefore, an open research question. Note that an instrument to measure turbulence uses the phase curvature of light [113].

*2) Biomedical Perspective: Imaging Through Turbid or Diffuse Media:* The use of optical biomedical imaging is an area that has seen tremendous growth in recent decades. Comparing the difficulty of imaging through living tissue with that of the ocean leads to the conclusion that the underwater imagers are quite fortunate, although that is not necessarily their perspective. A review paper [12] presents a wealth of information in addition to offering a somewhat different perspective on much the same physics. A document that considers the various mathematical formulations for diffusion imaging is [114]. Diffuse imaging plays an important role in the biomedical case because the absorption can range between 0.03 and 0.007 1/cm and the mean free path for scattering can be on the order of 100 $\mu$m, leading to a ratio of scattering to absorption of at least 2000.

As considered [12], photons that are either reflected from a target or imaged after passing through a media can be either ballistic, corresponding to the direct component above, or diffuse, in which case they are multiply scattered by the intervening medium. This case corresponds to that of multiple scatter that is relatively uncommon in underwater imaging as the single scatter albedo is much lower in underwater imaging. However, the case of "snake imaging," which is intermediate to these two cases, occurs when the scatter is predominately the forward scatter, which is certainly the case in underwater (UW) imaging.

Incoherent gated imaging is a technique that can separate the diffuse scatter from the ballistic photons when the path lengths and corresponding temporal differences are sufficient enough to permit separation. This can be extremely difficult for the short ranges considered, even though the path lengths may consist of many mean free paths. A temporal resolution of 100 fs may, indeed, be necessary in the biomedical case. A variety of techniques, some common to underwater imaging such as streak cameras, fast avalanche photodiodes, or gated optical image intensifiers are used. Other methods are harmonic generation, parametric amplification, the optical Kerr effect, and stimulated Raman scattering.

An alternative approach, to use coherent gating techniques, has been quite successful. Here, a heterodyne detection is used to detect the weak ballistic signals. As above, OCT has been used to image a variety of biological tissues both *in vitro* and *in vivo* from retina to gastrointestinal tract [115]. However, in this case, since the coherent detection is done in the time domain, scanning on a point-by-point basis is necessary to achieve the desired resolution. This may result in long scanning times (seconds) to achieve the desired spatial coverage in the biomedical case. A more recent technique, single shot or parallel OCT, uses quadrature detection of a set of four images on a CCD array, allowing phase coherent imaging [116]. However, the images are very much corrupt by speckle, as is true of most holograms, due to the coherent nature of the imaging process [117]. The potential use of OCT techniques to aid in under-

TABLE I
RESULT OF COMPUTING THE NUMBER OF POTENTIALLY ACHIEVABLE ATTENUATION LENGTHS FOR THE ROUND-TRIP IMAGING FROM (5)

| Input Power (Watts) | Total No. Atten. Lengths |
|---|---|
| $10^{-6}$ | 11.7 |
| $10^{-3}$ | 15.1 |
| 1 | 18.6 |

water imaging, although of academic interest, would ultimately be limited by the retention of the coherence between adjacent elements during propagation. Based on Caimi's results, considered above, one would have justification for a suspect attitude in using this method to achieve enhanced underwater imaging performance.

*3) Advanced Methodologies:* In this section, a number of more advanced technologies are considered to aid in underwater imaging. Topics range from the ultimate limitations imposed by the physics to the use of more advanced hardware and software for processing. A natural question that should be asked by those seeking to image underwater is: What is the ultimate limit to the process? As considered, the answer to this question can be found in considering the contrast transmittance, as given in several examples. To date, the standard assumption has been that several hundred photons are needed per pixel to form an acceptable image. One can compute, via simple analysis, a limit to visibility for a scanned system that images one pixel at a time. So, given approximately 200 photons of shot noise, the ultimate limit would imply an SNR of $200/\sqrt{200} \simeq 14$. Since 1 W of 532-nm green light corresponds to $2.6747 \times 10^{18}$ photons, the equation that governs the SNR for a single pixel, assuming that only ballistic photons are used in the image process, is

$$200 = I \times 2.67 \times 10^{18} e^{-2al} \rightarrow 37 + \ln(I) = 2 \times al \quad (5)$$

where $al$ is the number of total attenuation lengths that lead to useful images.

The results contained in Table I indicate that systems, considering only absorption-based imaging and assuming 100% collection of the reflected photons, should be able to image at close to 12 attenuation lengths. However, since the VSF for underwater targets is quite forward pointed, it is not unreasonable to assume that some fraction of those photons, especially after reflection from the target, will be useful. Since no underwater imaging system has achieved the performance as listed in this table, it appears as if there is some room for improvement.

A recent paper [118] may, in fact, render the idea that a few hundred photons are necessary as overly conservative. Here, the authors show that a range-gated system can provide adequate 3-D images with many fewer photons if more advanced processing techniques are used. However, the exact method used does require multiple exposures so that counting large numbers of photons is converted to a probability of arrival.

Another option is to increase the power via pulse compression technology. This technique, popular in both sonar and radar for some time now, propagates a time-varying signal that is followed by a correlator. The "pulse compression gain" or increase in the power in the height of the postcorrelated energy to that of the native signal is equal to the time–bandwidth product. In the case of a recently created chaotic laser [119], the gain is (3 GHz $\times$ 200 ns) $=$ 600 with a resolution of less than 1 cm. In the case of perfect correlation, the power in the original 150 mW (over 200 ns) will become 18 $\mu$J, a reasonable value as described above, and is also known to provide adequate power with efficient enough receiving apparatus.

In the realm of advanced signal processing, the development of compressive sensing deserves mention. The method uses a simplified detector with additional complexity in the transmitted signal geometry [120], [121]. Computational imaging with multiple cameras has also achieved some degree of success, albeit in synthetic situations [122].

## V. CONCLUSION

In this paper, the progression of underwater optical imaging from animal vision to modern laser scanning systems has been reviewed. As discussed, while the environment places fundamental limitations on both the range and the contrast of objects seen through the water, the potential for achieving the theoretical maximal physically permissible limits has not yet been achieved. Moreover, there is constant surprise as new technologies and imaging modalities are invented. For example, one could not have imagined forming range images with as few photons as described in [118] or as simple a detector architecture as described in [120].

A substantial challenge for future generations is to develop imaging systems that can eliminate the forward scatter, while, at the same time, imaging either a volume (via temporal signal range processing) or a simple 2-D image, nearly instantaneously. The technique described in [69] may offer a starting point, where sequential images are obtained from a set of isolatable beams, emulating the laser line scan system, although, now in a parallel acquisition geometry.

There is no doubt that the continued proliferation of higher performance, less expensive technology in the electro–optical marketplace will continue, availing the underwater imager of more options, at less cost. Last, maybe even quantum physics can be used for remote sensing to increase underwater optical imaging system performance, as discussed in [123].

## ACKNOWLEDGMENT

The author would like to thank the many collaborators and engineers that he has worked with over the years. Among the engineers are E. Reuss, E. Fuchs, K. Moore, R. Glatts, P. Roberts, and B. Laxton.

## REFERENCES

[1] N. G. Jerlov, *Marine Optics*. Amsterdam, The Netherlands: Elsevier, 1976, ch. 1.
[2] F. J. Ayala, "Darwin's greatest discovery: Design without designer," *Proc. Nat. Acad. Sci.*, vol. 104, no. Suppl 1, pp. 8567–8573, 2007.
[3] J. Watson, "Subsea imaging and vision: An introduction," in *Subsea Optics and Imaging*, J. Watson and O. Zielinski, Eds. Amsterdam, The Netherlands: Elsevier, 2013, ch. 2, pp. 17–34.
[4] J. S. Jaffe, K. D. Moore, J. McLean, and M. P. M. P. Strand, "Underwater optical imaging: Status and prospects," *Oceanography*, vol. 14, no. 3, pp. 66–76, 2001.
[5] D. M. Kocak and F. M. Caimi, "The current art of underwater imaging with a glimpse of the past and vision of the future," *Mar. Technol. Soc. J.*, vol. 39, no. 3, pp. 5–26, 2005.

[6] F. D. M. Kocak, R. Dalgleish, F. M. Caimi, and Y. Y. Schechner, "A focus on recent developments and trends in underwater imaging," *Mar. Technol. Soc. J.*, vol. 42, no. 1, pp. 52–67, 2008.

[7] F. R. Dalgleish, A. K. Vuorenkosk, and B. Ouyang, "Extended-range undersea laser imaging: Current research status and a glimpse at future technologies," *Mar. Technol. Soc. J.*, vol. 47, no. 5, pp. 128–147, 2013.

[8] A. Gershun, *The Light Field*. Cambridge, MA, USA: MIT Press, 1939, ch. 2.

[9] K. S. Shifrin, *Physical Optics of Ocean Water*. New York, NY, USA: Springer-Verlag, 1988, ch. 1.

[10] C. D. Mobley, *Light and Water: Radiative Transfer in Natural Waters*. San Diego, CA, USA: Academic, 1994, vol. 592.

[11] T. D. Dickey, G. W. Kattawar, and K. J. Voss, "Shedding new light on light in the ocean," *Phys. Today*, vol. 64, no. 4, pp. 44–49, 2011.

[12] C. Dunsby and P. M. W. French, "Techniques for depth-resolved imaging through turbid media including coherence-gated imaging," *J. Phys. D, Appl. Phys.*, vol. 36, no. 14, pp. R207–227, 2003.

[13] N. G. Jerlov, "Optical oceanography," in *Oceanography Series*. Amsterdam, The Netherlands: Elsevier, 1968, vol. 5.

[14] R. A. Arnone, A. M. Wood, and R. W. Gould Jr., "Water mass classification," *Oceanography*, vol. 17, no. 2, pp. 14–15, 2004.

[15] T. J. Petzold, "Volume scattering functions for selected ocean waters," Visibility Lab., Scripps Inst. Oceanogr., La Jolla, CA, USA, SIO-REF-72-78, 1972.

[16] T. J. Petzold, "Volume scattering functions for selected ocean waters," Visibility Lab., Scripps Inst. Oceanogr., La Jolla, CA, USA, Final Rep., 1972, pp. 72–78.

[17] O. Mikkelsen and M. Pejrup, "The use of a LISST-100 laser particle sizer for in-situ estimates of floc size, density and settling velocity," *Geo-Marine Lett.*, vol. 20, no. 4, pp. 187–195, 2001.

[18] L. Karp-Boss, L. Azevedo, and E. Boss, "LISST-100 measurements of phytoplankton size distribution: Evaluation of the effects of cell shape," *Limnol. Oceanogr. Methods*, vol. 5, pp. 396–406, 2007.

[19] K. J. Voss and E. S. Fry, "Measurement of the Mueller matrix for ocean water," *Appl. Opt.*, vol. 23, no. 23, pp. 4427–4439, 1984.

[20] W. Hou, S. Woods, E. Jarosz, W. Goode, and A. Weidemann, "Optical turbulence on underwater image degradation in natural environments," *Appl. Opt.*, vol. 51, no. 14, pp. 2678–2686, 2012.

[21] W. W. Hou, "A simple underwater imaging model," *Opt. Lett.*, vol. 34, no. 17, pp. 2688–2690, 2009.

[22] S. Johnsen, "Transparent animals," *Sci. Amer.*, vol. 282, no. 2, pp. 62–71, 2000.

[23] J. T. O. Kirk, *Light and Photosynthesis in Aquatic Ecosystems*. Cambridge, U.K.: Cambridge Univ. Press, 1994.

[24] J. Wei, R. V. Dommelen, M. R. Lewis, S. McLean, and K. J. Voss, "A new instrument for measuring the high dynamic range radiance distribution in near-surface sea water," *Opt. Exp.*, vol. 20, no. 24, pp. 27024–27038, 2012.

[25] M. F. Land and D. E. Nilsson, *Animal Eyes*. Oxford, U.K.: Oxford Univ. Press, 2012, ch. 4.

[26] D. E. Nilsson, E. J. Warrant, S. Johnsen, R. Hanlon, and N. Shashar, "A unique advantage for giant eyes in giant squid," *Curr. Biol.*, vol. 22, no. 8, pp. 683–688, 2012.

[27] L. Dagorn, P. Bach, and E. Josse, "Movement patterns of large bigeye tuna (Thunnus obesus) in the open ocean, determined using ultrasonic telemetry," *Mar. Biol.*, vol. 136, no. 2, pp. 361–371, 2000.

[28] T. W. Cronin and N. J. Marshall, "A retina with at least ten spectral types of photoreceptors in a mantis shrimp," *Nature*, vol. 339, no. 6220, pp. 137–140, 1989.

[29] J. Marshall and J. Oberwinkler, "Ultraviolet vision: The colourful world of the mantis shrimp," *Nature*, vol. 401, no. 6756, pp. 873–874, 1999.

[30] J. N. Lythgoe, "Polarized light and underwater vision," *Nature*, vol. 213, pp. 893–894, 1967.

[31] T. H. Waterman, "Reviving a neglected celestial underwater polarization compass for aquatic animals," *Biol. Rev.*, vol. 81, no. 1, pp. 111–115, 2006.

[32] Y. Y. Schechner and N. Karpel, "Clear underwater vision," in *Proc. IEEE Comput. Soc. Conf. Comput. Vis. Pattern Recognit.*, 2004, vol. 1, pp. 536–543.

[33] N. Shashar, R. T. Hanlon, and A. deM. Petz, "Polarization vision helps detect transparent prey," *Nature*, vol. 393, no. 6682, pp. 222–223, 1998.

[34] J. Marshall, T. W. Cronin, N. Shashar, and M. Land, "Behavioral evidence for polarization vision in stomatopods reveals a potential channel for communication," *Curr. Biol.*, vol. 9, no. 14, pp. 755–758, 1999.

[35] F. H. Spiess and R. C. Tyce, "Marine Physical Laboratory deep tow instrumentation system Mar. Phys. Lab, Scripps Inst. Oceanogr., San Diego, CA, USA, Rep. SIO-Ref-73-4, 1973.

[36] R. D. R. D. Ballard, "The history of Woods Hole's deeps submergence program," in *50 Years of Ocean Discovery: National Science Foundation 1950–2000*. Washington, DC, USA: National Academies Press, 2000, pp. 67–84.

[37] C. Luiggi, "Life on the ocean floor, 1977," *The Scientist*, Sep. 2012.

[38] S. S. Harris and R. D. Ballard, "ARGO: Capabilities for deep ocean exploration," in *Proc. OCEANS Conf.*, 1986, pp. 6–8.

[39] S. Q. Duntley, "Light in the sea," *J. Opt. Soc. Amer.*, vol. 53, no. 2, pp. 214–233, 1963.

[40] E. P. Zege, A. P. Ivanov, and I. L. Katsev, *Image Transfer through a Scattering Medium*. New York, NY, USA: Springer-Verlag, 1991, ch. 5.

[41] J. Graham, "Secchi disc observations and extinction coefficients in the Central and Eastern North Pacific Ocean," *Limnol. Oceanogr.*, vol. 11, no. 2, pp. 184–185, 1966.

[42] W. Hou, Z. Lee, and A. D. Weidemann, "Why does the Secchi Disk disappear? An imaging perspective," Oceanogr. Div., Naval Res. Lab., Stennis Space Center, MS, USA, NRL/JA/7330-06-7053, 2007.

[43] Zaneveld, J. Ronald, and W. Pegau, "Robust underwater visibility parameter," *Opt. Exp.*, vol. 11, no. 23, pp. 2997–3009, 2003.

[44] R. H. Blackwell, "Contrast thresholds of the human eye," *J. Opt. Soc. Amer.*, vol. 36, no. 11, pp. 624–643, 1946.

[45] T. W. Cronin, N. Shashar, R. L. Caldwell, J. Marshall, A. G. Cheroske, and T.-H. Chiou, "Polarization vision and its role in biological signaling," *Integr. Compar. Biol.*, vol. 43, no. 4, pp. 549–558, 2003.

[46] N. Shashar and T. W. Cronin, "Polarization contrast vision in octopus," *J. Exp. Biol.*, vol. 199, no. 4, pp. 999–1004, 1996.

[47] T. H. Waterman, "Polarization patterns in submarine illumination," *Science*, vol. 120, no. 3127, pp. 927–932, 1954.

[48] Y. Y. Schechner and N. Karpel, "Recovery of underwater visibility and structure by polarization analysis," *IEEE J. Ocean. Eng.*, vol. 30, no. 3, pp. 570–587, Jul. 2005.

[49] Y. Y. Schechner, "Inversion by $P^4$: Polarization-picture post-processing," *Philosoph. Trans. Roy. Soc. B, Biol. Sci.*, vol. 366, no. 1565, pp. 638–648, 2011.

[50] S. Chandrasekhar, *Radiative Transfer*. New York, NY, USA: Courier Dover, 1960.

[51] R. W. Preisendorfer, *Hydrologic Optics*. Washington, DC, USA: U.S. Dept. Commerce, Nat. Ocean. Atmos. Admin., Environ. Res. Labs, 1976, vol. 6.

[52] C. D. Mobley, "A numerical model for the computation of radiance distributions in natural waters with wind-roughened surfaces," *Limnol. Oceanogr.*, vol. 34, no. 8, pp. 1473–1483, 1989.

[53] C. D. Mobley, L. K. Sundman, and E. Boss, "Phase function effects on oceanic light fields," *Appl. Opt.*, vol. 41, no. 6, pp. 1035–1050, 2002.

[54] G. C. Chang, T. D. Dickey, E. Boss, C. D. Mobley, and W. S. Pegau, "Toward closure of upwelling radiance in coastal waters," *Appl. Opt.*, vol. 42, no. 9, pp. 1574–1582, 2003.

[55] M. Tzortziou *et al.*, "Bio-optics of the Chesapeake Bay from measurements and radiative transfer closure," *Estuar. Coast. Shelf Sci.*, vol. 68, pp. 348–362, 2006.

[56] S. K. Nayar, "Computational cameras: Redefining the image," *IEEE Computer*, vol. 39, no. 8, pp. 30–38, Aug. 2006.

[57] J. S. Jaffe, "Computer modeling and the design of optimal underwater imaging systems," *IEEE J. Ocean. Eng.*, vol. 15, no. 2, pp. 101–111, Apr. 1990.

[58] J. D. Foley and A. V. Dam, "Fundamentals of interactive computer graphics," in *Systems Programming Series*. Reading, MA, USA: Addison-Wesley, 1982, ch. 6.

[59] H. Zhang, K. J. Voss, R. P. Reid, and E. M. Louchard, "Bidirectional reflectance measurements of sediments in the vicinity of Lee Stocking Island, Bahamas," *Limnol. Oceanogr.*, vol. 48, no. 1, pt. 2, pp. 380–389, 2003.

[60] J. W. Goodman, "Introduction to Fourier optics," in *Introduction to Fourier Optics*, ser. Electrical and Computer Engineering; Electromagnetics, 2nd ed. New York, NY, USA: .McGraw-Hill, 1995, ch. 2, ISBN: 0070242542 1.

[61] B. L. McGlamery, "A computer model for underwater camera systems," in *Ocean Optics VI*. Philadelphia, PA, USA: SPIE, 1980, pp. 221–231.

[62] H. R. Gordon, "Equivalence of the point and beam spread functions of scattering media: A formal demonstration," *Appl. Opt.*, vol. 33, no. 6, pp. 1120–1122, 1994.

[63] J. S. Jaffe, "Monte Carlo modeling of underwater-image formation: Validity of the linear and small-angle approximations," *Appl. Opt.*, vol. 34, no. 24, pp. 5413–5421, 1995.

[64] J. S. Jaffe, "Performance bounds on synchronous laser line scan systems," *Opt. Exp.*, vol. 13, no. 3, pp. 738–748, 2005.

[65] T. Wilson, "Scanning optical microscopy," *Scanning*, vol. 7, no. 2, pp. 79–87, 1985.

[66] K. D. Moore, J. S. Jaffe, and B. L. Ochoa, "Development of a new underwater bathymetric laser imaging system: L-Bath," *J. Atmos. Ocean. Technol.*, vol. 17, no. 8, pp. 525–545, 2000.

[67] M. P. Strand, B. Coles, A. J. Nevis, and R. F. Regan, "Laser line scan fluorescence and multispectral imaging of coral reef environments," *Proc. SPIE—Int. Soc. Opt. Eng.*, vol. 2963, pp. 790–795, 1997.

[68] J. D. Broadwater and D. John, *USS Monitor: A Historic Ship Completes its Final Voyage*. College Station, TX, USA: Texas A&M Univ. Press, 2012, p. 68.

[69] J. S. Jaffe, "Enhanced extended range underwater imaging via structured illumination," *Opt. Exp.*, vol. 18, no. 12, pp. 12328–12340, 2010.

[70] R. W. Austin, S. Q. Duntley, R. L. Ensminger, T. J. Petzold, and R. C. Smith, "An underwater laser scanning system," *Proc. SPIE—Int. Soc. Opt. Eng.*, vol. 1537, pp. 57–73, 1991.

[71] L. Mullen, A. Laux, B. Cochenour, and W. McBride, "Extended range underwater imaging using a time varying intensity (TVI) approach," in *Proc. MTS/IEEE OCEANS Conf. Biloxi – Marine Technol. for Our Future: Global and Local Challenges*, 2009.

[72] J. H. Churnside, V. V. Tatarskii, and J. J. Wilson, "Airborne lidar for fisheries applications," *Opt. Eng.*, vol. 40, no. 3, pp. 406–414, 2001.

[73] G. R. Fournier, D. Bonnier, J. L. Forand, and P. W. Pace, "Range-gated underwater laser imaging system," *Opt. Eng.*, vol. 32, no. 9, pp. 2185–2190, 1993.

[74] J. W. McLean, "High-resolution 3D underwater imaging," in *Proc. SPIE Int. Symp. Opt. Sci. Eng. Instrum.*, 1999, pp. 10–19.

[75] A. D. Gleckler, "Multiple-slit streak tube imaging lidar (MS-STIL) applications," *Proc. SPIE—Int. Soc. Opt. Eng.*, vol. 4035, pp. 266–278, 2000.

[76] J. S. Jaffe, *Personal Communication.* 2014.

[77] L. Mullen *et al.*, "Modulated laser line scanner for enhanced underwater imaging," in *Proc. SPIE Int. Symp. Opt. Sci. Eng. Instrum.*, 1999, pp. 2–9.

[78] L. Mullen *et al.*, "Amplitude-modulated laser imager," *Appl. Opt.*, vol. 43, no. 19, pp. 3874–3892, 2004.

[79] B. Cochenour, S. O'Connor, and L. Mullen, "Suppression of forward-scattered light using high-frequency intensity modulation," *Opt. Eng.*, vol. 53, no. 5, 2014, 051406.

[80] P. B. Ortner, S. R. Cummings, R. P. Aftring, and H. E. Edgerton, "Silhouette photography of oceanic zooplankton," *Nature*, vol. 277, pp. 50–51, 1979.

[81] P. B. Ortner, L. C. Hill, and H. E. Edgerton, "In-situ silhouette photography of Gulf Stream zooplankton," *Deep Sea Res. A, Oceanogr. Res. Papers*, vol. 28, no. 12, pp. 1569–1576, 1981.

[82] S. G. Settles, *Schlieren and Shadowgraph Techniques*. New York, NY, USA: Springer-Verlag, 2001, ch. 6.

[83] P. H. Wiebe and M. C. Benfield, "From the Hensen net toward four-dimensional oceanography," *Progr. Oceanogr.*, vol. 56, pp. 7–136.

[84] K. L. Carder, "Holographic microvelocimeter for use in studying ocean particle dynamics," *Opt. Eng.*, vol. 18, no. 5, pp. 524–525, 1979.

[85] K. L. Carder, R. G. Steward, and P. R. Betzer, "In situ holographic measurements of the sizes and settling rates of oceanic particulates," *J. Geophys. Res., Oceans (1978–2012)*, vol. 87, no. C8, pp. 5681–5685, 1982.

[86] J. Katz, S. Gowing, T. O'Hern, and A. Acosta, "A comparative study between holographic and light-scattering techniques of microbubble detection," in *Measuring Techniques in Gas-Liquid Two-Phase Flows*. Berlin, Germany: Springer-Verlag, 1984., pp. 41–66.

[87] R. B. Owen and A. A. Zozulya, "In-line digital holographic sensor for monitoring and characterizing marine particulates," *Opt. Eng.*, vol. 39, no. 8, pp. 2187–2197, 2000.

[88] H. P. Sun *et al.*, "Underwater digital holography for studies of marine plankton," *Philosoph. Trans. Roy. Soc. A, Math. Phys. Eng. Sci.*, vol. 366, no. 1871, pp. 1789–1806, 2008.

[89] G. W. Graham and W. M. Nimmo-Smith, "The application of holography to the analysis of size and settling velocity of suspended cohesive sediments," *Limnol. Oceanogr., Methods*, vol. 8, pp. 1–15, 2009.

[90] J. S. Jaffe, P. J. S. Franks, C. Briseno, P. L. D. Roberts, and B. Laxton, "Advances in underwater fluorometry, from bulk fluorescence to planar laser imaging of individuals," in *Subsea Optics and Imaging*, J. Watson and O. Zielinski, Eds. Cambridge, U.K.: Woodhead, 2013, ch. 17.

[91] G. Gorsky *et al.*, "Digital zooplankton image analysis using the ZooScan integrated system," *J. Plankton Res.*, vol. 32, no. 3, pp. 285–303, 2010.

[92] M. E. Sieracki *et al.*, "Optical plankton imaging and analysis systems for ocean observation," in *Proc. OceanObs'09: Sustained Ocean Observations and Information for Society*, J. Hall, D. E. Harrison, and D. Stammer, Eds., Venice, Italy, Sep. 21–25, 2009, vol. 2, pp. 21–25, ESA Publication WPP-306.

[93] J. S. Jaffe, P. J. S. Franks, and A. W. Leising, "Simultaneous imaging of phytoplankton and zooplankton distributions," *Oceanography*, vol. 11, no. 1, pp. 24–29, 1998.

[94] P. J. S. Franks and J. S. Jaffe, "Microscale distributions of phytoplankton: Initial results from a two-dimensional imaging fluorometer, OSST," *Mar. Ecol. Progr. Ser.*, vol. 220, pp. 59–72, 2001.

[95] A. W. Palowitch and J. S. Jaffe, "Three-dimensional ocean chlorophyll distributions from underwater serial-sectioned fluorescence images," *Appl. Opt.*, vol. 33, no. 14, pp. 3023–3033, 1994.

[96] A. W. Palowitch and J. S. Jaffe, "Optical serial sectioned chlorophyll a microstructure," *J. Geophys. Res., Oceans (1978–2012)*, vol. 100, no. C7, pp. 13267–13278, 1995.

[97] J. C. Prairie, P. J. S. Franks, and J. S. Jaffe, "Cryptic peaks: Invisible vertical structure in fluorescent particles revealed using a planar laser imaging fluorometer," *Limnol. Oceanogr.*, vol. 55, no. 5, pp. 1943–1958, 2010.

[98] J. C. Prairie, P. J. S. Franks, J. S. Jaffe, M. J. Doubell, and H. Yamazaki, "Physical and biological controls of vertical gradients in phytoplankton," *Limnol. Oceanogr., Fluids Environ.*, vol. 1, pp. 75–90, 2011.

[99] D. Zawada, "The application of a novel multispectral imaging system to the in vivo study of fluorescent compounds in selected marine organisms," Ph.D. dissertation, Scripps Inst. Oceanogr., Univ. California San Diego, La Jolla, CA, USA, 2002.

[100] E. F. DeLong and F. Edward, "The microbial ocean from genomes to biomes," *Nature*, vol. 459, no. 7244, pp. 200–206, 2009.

[101] D. M. Anderson, P. M. Gilbert, and J. M. Burkholder, "Harmful algal blooms and eutrophication: Nutrient sources, composition, and consequences," *Estuaries*, vol. 25, no. 4, pp. 704–726, 2002.

[102] R. J. Olson and H. M. Sosik, "A submersible imaging-in-flow instrument to analyze nano-and microplankton: Imaging FlowCytobot," *Limnol. Oceanogr., Methods*, vol. 5, pp. 195–203, 2007.

[103] H. M. Sosik and R. J. Olson, "Automated taxonomic classification of phytoplankton sampled with imaging-in-flow cytometry," *Limnol. Oceanogr., Methods*, vol. 5, pp. 204–216, 2007.

[104] J. Sheng, E. Malkiel, and J. Katz, "Digital holographic microscope for measuring three-dimensional particle distributions and motions," *Appl. Opt.*, vol. 45, no. 16, pp. 3893–3901, 2006.

[105] J. Sheng *et al.*, "Digital holographic microscopy reveals prey-induced changes in swimming behavior of predatory dinoflagellates," *Proc. Nat. Acad. Sci.*, vol. 104, no. 44, pp. 17512–17517, 2007.

[106] S. Talapatra *et al.*, "Characterization of biophysical interactions in the water column using in situ digital holography," *Mar. Ecol. Progr. Ser.*, vol. 473, pp. 29–51, 2013.

[107] J. Garcia-Sucerquia *et al.*, "Digital in-line holographic microscopy," *Appl. Opt.*, vol. 45, no. 5, pp. 836–850, 2006.

[108] Cheong *et al.*, "Flow visualization and flow cytometry with holographic video microscopy," *Opt. Exp.*, vol. 17, no. 15, pp. 13071–13079, 2009.

[109] T. Triebitz, *Personal Communication.* 2014.

[110] K. A. Stetson, "Holographic fog penetration," *J. Opt. Soc. Amer.*, vol. 57, no. 8, pp. 1060–1062, 1967.

[111] W. J. Stachnik, "The measurement of optical coherence loss in Atlantic waters," in *Proc. 22nd Annu. Tech. Symp. Int. Soc. Opt. Photon.*, 1978, pp. 154–165.

[112] F. M. Caimi, B. C. Bailey, and J. H. Blatt, "Undersea object detection and recognition: The use of spatially and temporally varying coherent illumination," in *Proc. MTS/IEEE OCEANS Conf., Riding the Crest into the 21st Century"*, 1999, vol. 3, pp. 1474–1479.

[113] D. J. Bogucki, J. A. Domaradzki, C. Anderson, H. W. Wijesekera, R. V. Zaneveld, and C. Moore, "Optical measurement of rates of dissipation of temperature variance due to oceanic turbulence," *Opt. Exp.*, vol. 15, no. 12, pp. 7224–7230, 2007.

[114] S. R. Arridge and J. Schotland, "Optical tomography: Forward and inverse problems," *Inverse Probl.*, vol. 15, pp. R41–R93, 1999.

[115] A. F. Fercher, W. Drexler, C. K. Hitzenberger, and T. Lasser, "Optical coherence tomography-principles and applications," *Rep. Progr. Phys.*, vol. 66, no. 2, pp. 239–303, 2003.

[116] M. S. Hrebesh, R. Dabu, and M. Sato, "*In vivo* imaging of dynamic biological specimen by real-time single-shot full-field optical coherence tomography," *Opt. Commun.*, vol. 282, no. 4, pp. 674–683, 2009.
[117] J. W. Goodman, *Statistical Optics*. New York, NY, USA: Wiley-Interscience, 1985, p. 567.
[118] A. Kirmani *et al.*, "First-photon imaging," *Science*, vol. 343, no. 6166, pp. 58–61, 2014.
[119] L. K. Rumbaugh, E. M. Bollt, W. D. Jemison, and Y. Li, "A 532 nm chaotic lidar transmitter for high resolution underwater ranging and imaging," in *Proc. OCEANS Conf.*, 2013.
[120] B. Ouyang *et al.*, "Compressive sensing underwater laser serial imaging system," *SPIE J. Electron. Imag.*, vol. 22, Special Edition on Compressive Sensing, no. 2, Apr. 2013, DOI: 10.1117/1.JEI.22.2.021010.
[121] B. Ouyang *et al.*, "Compressive line sensing underwater imaging system," *Opt. Eng.*, vol. 53, no. 5, 2014, 051409.
[122] M. Levoy, B. Chen, V. Vaish, M. Horowitz, I. McDowall, and M. Bolas, "Synthetic aperture confocal imaging," *ACM Trans. Graph.*, vol. 23, no. 3, pp. 825–834, 2004.
[123] A. Gatti, E. Brambilla, and L. A. Lugiato, "Entangled imaging and wave-particle duality: From the microscopic to the macroscopic realm," *Phys. Rev. Lett.*, vol. 90, no. 13, 2003, 133603.

**Jules S. Jaffe** (A'85) received the B.A. degree in physics from the State University of New York at Buffalo, Buffalo, NY, USA, in 1973, the M.S. degree in biomedical information science from the Georgia Institute of Technology, Atlanta, GA, USA, in 1974, and the Ph.D. degree in biophysics from the University of California at San Diego, La Jolla, CA, USA, in 1982.

He subsequently spent several years in Silicon Valley as an image-processing consultant. In 1984, he joined the Woods Hole Oceanographic Institution, Woods Hole, MA, USA, where he worked as an Assistant and Associate Scientist. In 1988, he joined the Scripps Institution of Oceanography, University of California at San Diego, as an Assistant Research Oceanographer. He was subsequently promoted to Associate and then Full Oceanographer, which is his current position. His lab specializes in the development of a variety of underwater technology that ranges from miniature vehicles to underwater optical and acoustical instruments. In 2003, he was a visiting H. Burr Steinbuck Visiting Scholar at the Woods Hole Oceanographic Institution. In 2006, he was a Visiting Miller Professor at the University of California, Berkeley.

Dr. Jaffe is a Fellow of the Acoustical Society and a past recipient of a National Science Foundation Creativity Award. In 2012, he won a "best paper award" at the International Ocean Optics Meeting. He is currently an Associate Editor of the IEEE JOURNAL OF OCEANIC ENGINEERING, and he recently started a new journal: *Methods in Oceanography* (Elsevier) as Editor-in-Chief.